INVESTIGATING INORGANIC ARSENIC EXPOSURE AND CARDIAC HYPERTROPHY

by

Raihan Kabir

A thesis submitted to Johns Hopkins University in conformity with the requirements for the degree of Master of Science.

Baltimore, Maryland

April 2020

ABSTRACT

Objective

Arsenic exposure through drinking water is well-associated with adverse cardiovascular outcomes, yet the pathophysiological mechanisms by which inorganic arsenic (iAS) induces these effects are largely unknown. Recently, an epidemiological study found that iAS exposure was associated with altered left ventricular geometry. Considering the possibility that iAS directly induces cardiac remodeling independent of hypertension, we investigated the impact of an environmentally relevant iAS exposure on the structure and function of male and female hearts.

Methods and Results

Adult male and female C56BL/6J mice were exposed to 615 μg/L $NaAsO_2$ for eight weeks. Males exhibited increased systolic blood pressure via tail cuff photoplethysmography, left ventricular wall thickness via transthoracic echocardiography, and increased plasma atrial natriuretic peptide via enzyme immunoassay. RT-qPCR revealed increased myocardial RNA transcripts of *Acta1*, *Myh7*, and *Nppa*, and decreased *Myh6*, providing evidence of pathological hypertrophy in the male heart. Similar changes were not observed in females at the same eight-week timepoint supporting the existence of a cardioprotective mechanism, but we did observe evidence that this protective signaling is starting to decline. Further investigation elucidated the upregulation of *Rcan1* with iAS exposure in male hearts. We also observed iAS to directly activate NFAT in HEK293 cells using a luciferase assay, indicating that iAS exposure may induce pathological cardiac hypertrophy in part by targeting the calcineurin-NFAT pathway.

Conclusions

Overall, this investigation provides the first mechanistic link between an environmentally relevant dose of iAS and the induction of pathological hypertrophy in the heart. We also found that iAS directly activates calcineurin-NFAT signaling in vitro, in accordance with findings that highlight an association between iAS exposure and cardiac remodeling in populations with a low burden of cardiovascular risk factors. Chronic iAS exposure is widespread, and these results provide biological impetus for its removal from human consumption.

Keywords

Inorganic Arsenic Exposure; Environmental Exposure; Blood Pressure; Cardiac Hypertrophy; Sex Differences; Calcineurin-Nuclear Factor of Activated T-Cells

Thesis Advisor

Mark J. Kohr, PhD, FAHA, FCVS

Thesis Reader

Winnie Wan-Yee Tang, PhD

ACKNOWLEDGEMENTS اَلْحَمْدُ لله

Special appreciation is necessary. Thank you:

Dr. Mark Kohr for fostering my growth as a young scientist.

Dr. Winnie Tang and Dr. Oby Ebenebe for serving as intellectual guides.

Prithvi Sinha and Nicole Taube for providing expansive support.

And undying gratitude to my parents, Mahmuda Akhter Kabir & Sheikh Humayun Kabir.

TABLE OF CONTENTS

LIST OF FIGURES

CHAPTER 1

BACKGROUND

1.0 General Introduction

Human need to meet the energy demands of physical exertion has evolutionarily selected the modern *Homo sapiens* cardiovascular system.[1] Continuous circulation of oxygen, hormones, and nutrients throughout the body is achieved through its intricate coordination of heart, vasculature, and blood. Proper functioning of this system is dependent upon an unperturbed harmony, else an individual becomes pre-disposed to cardiovascular disease (CVD), the world's leading cause of death.[2] Traditionally, risk factors for CVD have been considered unisex and modifiable such that the notions of increasing physical activity and potassium intake, decreasing smoking and sodium intake, and adhering to dietary approaches to stop hypertension are recommended to the general public.[3] However, an awareness that there exists a greater age-adjusted CVD mortality rate among males compared to premenopausal females has shifted clinical care to recognize sex-specific symptoms and promote their respective recommendations for disease prevention.[4] Currently, environmental agents such as metals and air pollution are implicated in CVD etiology and pathogenesis.[5] Growing evidence suggests that these exposures initiate and augment pathophysiological processes in a manner similar to that of traditional risk factors.[5] Analogous to recent developments in understanding sex differences in CVD, investigation of the biological bases of environmental exposures' potentially sex-disparate effects on health and well-being has become necessary. Exploration of the mechanisms by which inorganic arsenic exposure alters the structure and function of the heart in this thesis is thus a modest effort to promote health and well-being.

1.1 Heart Physiology

Mammalians hearts are comprised of four distinct muscular chambers, two atria and two ventricles, which are divided into the functionally separate right and left sides of the heart; the right atrium and ventricle pump blood from the inferior and superior vena cava to the pulmonary arteries for oxygenation, and the left atrium and ventricle pump this oxygenated blood from the pulmonary veins to the aorta for systemic circulation. Four distinct valves isolate and ensure unidirectional flow between atrial chambers and their respective ventricles (the tricuspid and mitral valves for the right and left heart, respectively), as well as ventricular chambers and their respective arterial systems (the pulmonary and aortic valves). Opening and closing of all such valves is primarily dictated by the pressure gradient across the valve, which becomes a concern, for example, when systemic blood pressure is consistently outside of the normal physiological range. Hearts are primarily composed of cardiac muscle cells, termed cardiomyocytes; these cells are electrically excitable and generate action potentials to orchestrate chamber contraction based on both time- and voltage-dependent changes in transmembrane ion channels. Cardiomyocytes differ in their action potential characteristics based on their role in (1) regulating the heart rate as pacemaker cells, (2) synchronizing the different regions of the heart in the Purkinje network, (3) contracting the atrial cambers, or (4) contracting the ventricles. Following cardiomyocyte depolarization in all contracting cells, potassium efflux is balanced by an influx of calcium ions through L-type calcium channels, the duration of which depends on the role of the cell. Calcium then enters cardiomyocytes and induces further calcium release from the sarcoplasmic reticulum; these calcium ions diffuse through myofilament lattice and bind to an inhibitory troponin protein, which allows actin-myosin interactions, resulting in contraction. Considering that the rhythmic contraction (systole) and relaxation (diastole) of the myocardium—the muscular tissue of the heart—is

intricately regulated not only by the filling and ejection of blood but also by electrical signals and the cycling of intracellular calcium, the dysfunction of any such part may result in an array of cardiac pathologies.

1.1.1 Cardiovascular Disease

Pathologies related to the cardiovascular system constitute the largest global burden of disease.[6,7] Among these pathologies, coronary heart disease, high blood pressure, and heart failure contribute to the majority of CVD-attributable deaths.[8] Coronary arteries are blood vessels that supply the myocardium, and as such, coronary heart disease is characterized by the insufficient delivery of oxygenated blood to the heart—also termed ischemic heart disease. Heart failure, on the other hand, is broadly characterized by abnormalities in the myocardium that may impair pressure development or relaxation, resulting in either a preserved or reduced amount of blood ejected from the heart, termed ejection fraction. Beyond the palpable adverse health effects inflicted on the individuals experiencing these pathologies, CVD results in a significant economic burden by not only generating tremendous healthcare costs, but also by decreasing worker productivity.

1.1.2 Sex Differences in Heart Physiology and Pathology

Fundamental heart functions are maintained across both biological sexes, defined by chromosomal composition, but there exist several recently appreciated differences in cardiac physiology and CVD pathology between males and females.

Sex differences in the heart begin to manifest at puberty as the concentration of sex steroids and the expression of their respective receptors begin to increase.[9] Estrogen and testosterone are present in both sexes but are found at higher levels in females and males, respectively.

Classically, estrogen and its major circulating compound, 17beta-estradiol, can function by binding to nuclear receptors, estrogen receptor alpha and estrogen receptor beta, and acting as a transcription factor complex to then directly regulate the expression of target estrogen-responsive genes; the estrogen-receptor complex can also interact with other classes of transcription factors to regulate the expression of genes without estrogen-responsive elements in their promoter regions.[10] Testosterone can similarly bind nuclear receptors to modulate genomic actions; it is worth noting here that testosterone may be converted to estrogen by aromatase. However, estrogen can alternatively function by interacting with membrane receptors and signaling cascades to modulate non-genomic actions.[10] Nonetheless, both classes of sex steroids are thought to construct their respective sex-based differences in heart physiology and CVD outcomes.

Pre-menopausal females generally exhibit better cardiac function at baseline compared to age-matched males.[9] Anatomically, male hearts have greater mass compared to female hearts, and this is mediated not by an increase in the number of cardiomyocytes, but by an increase in cardiomyocyte size—hypertrophy—throughout the male heart.[9] Additionally, studies on male and female response to physiological cardiovascular stress, such as exercise, do not find a difference in cardiac output, which is a function of heart rate and the amount of blood pumped with each heartbeat, termed stroke volume.[11,12] Rather, sex differences in this context manifest in the respective mechanism of increasing cardiac output; whereas males increase their total peripheral vascular resistance, females predominantly increase their heart rate.[13] Furthermore, the female cardiovascular system is uniquely equipped to increase cardiac output and decrease blood pressure to meet the metabolic needs of pregnancy.[14] Beyond a distinguished response to physiological events, females are also found to have endogenous protection against adverse cardiac pathologies, which is not found in their male

counterparts. Pre-menopausal females have a lower prevalence of ischemic heart disease and heart failure compared to age-matched males, and this is thought to be partially attributable to estrogen.[15,16] Estrogen has been shown to activate protective mechanisms involving calcium handling, which regulates cardiac electrophysiology and contraction; phosphoinositol 3-kinase (PI3K) and Akt, which regulate cell survival pathways; and nitric oxide (NO), which regulates signaling in cardiomyocytes and endothelium.[9] Molecular sex differences that extend into cardiovascular redox biology continue to be unraveled, highlighting the importance of accounting for sex and hormonal status in studying the heart in health and disease.[17]

1.2 Cardiac Hypertrophy

1.2.1 Physiological Hypertrophy and PI3K-Akt Signaling

Cardiac remodeling describes post-gestational alterations in the structure of the myocardium. Females undergo cardiac remodeling during pregnancy, for example, to enlarge the ventricles of the heart and facilitate an increase in cardiac output. Repetitive endurance exercise can also induce hypertrophic growth of the myocardium; this occurs as a compensatory, adaptive mechanism to counterbalance the increased ventricular wall tension, induced by elevated blood pressure, and meet metabolic demands. During such growth, termed physiological hypertrophy, there is an increase in cardiac mass as a result of cardiomyocyte enlargement in both width and length, as well as a proportional expansion of the capillary network supplying the myocardium via angiogenesis, such that normal cardiac function is maintained.

Physiological hypertrophy is coordinated by an array of molecular responses to promote energy production, cardiomyocyte proliferation, antioxidant systems, and protein quality

control. Signals from mechano-transduced forces and growth hormones, such as insulin, trigger cell survival pathways, including the PI3K and Akt cascade. Insulin binds to the insulin receptor, which is a tyrosine kinase that phosphorylates insulin receptor substrate adaptor proteins to activate PI3K, generating phosphatidylinositol 3,4,5-triphosphate (PIP_3) and thereby phosphorylating and activating Akt to coordinate protein synthesis and cell growth. Moreover, PI3K signaling exhibits crosstalk with the expansive mitogen-activation protein kinase (MAPK) pathway, which can coordinate transcriptional regulation to promote physiological hypertrophy. Insulin-like growth factor 1 (IGF1), which is synthesized and secreted in the heart upon growth hormone stimulation, can act through its own receptor to also canonically activate the Akt and MAPK pathways. Several studies have demonstrated that the promotion of Akt expression and activation by transgenic alteration of upstream mediators such as PI3K or IGF1 was responsible for myocardial growth without cardiac dysfunction.[18–20] Considering that several pathways share Akt as a downstream effector of adaptive processes, levels of Akt gene and protein expression as well as phosphorylation, serve as strong markers of physiological hypertrophy. Beyond PI3K and Akt signaling, the IGF1 receptor can activate a heterotrimeric G protein subunit to activate phospholipase C (PLC) and generate inositol 1,4,5-triphosphate (IP3) to induce the release of calcium from the endoplasmic and sarcoplasmic reticulum and facilitate cardiomyocyte contraction. Taken together, these processes, among others, direct an adaptive response in cardiac performance to meet the structural and metabolic demands of physiological hemodynamic stress.

1.2.2 Pathological Cardiac Hypertrophy and Calcineurin-NFAT

Although cardiac remodeling may be adaptive as described, adverse stress such as ischemic injury, cardiomyocyte loss, or hemodynamic overload can drive pathological hypertrophy of

the heart. Chronic hypertension, which describes a consistently elevated blood pressure exceeding a defined range, confers greater pressure on the myocardium that it must overcome in order to proceed with each circulatory pump; hypertensive left ventricular hypertrophy may thus result in order to meet this demand. However, in this pathological context, cardiomyocyte growth is asymmetric and exceeds the capacity of the capillary network supplying the myocardium. Geometrically, pathological hypertrophy may either be concentric, characterizing an increased wall thickness and decreased ventricular chamber as a result of cardiomyocyte expansion in thickness rather than length, or eccentric, describing a dilated ventricular chamber as a result of cardiomyocyte expansion in length. Whereas an adaptive response following Laplace's law accounts for an increase in ventricular pressure by an inversely proportional increase in ventricular wall thickness, eccentric remodeling instead increases the cavity radius, proportional to ventricular wall stress. Although concentric hypertrophy can progress into eccentric hypertrophy, or vice versa via clinical intervention targeting mechanical unloading, cardiac dysfunction manifests in both maladaptive classes as a result of altered calcium handling, sarcomere disorganization, metabolic dysregulation, fibrosis, and cardiomyocyte death.[21] Appropriately, pathological cardiac hypertrophy is characterized as an independent risk factor for adverse cardiovascular events such as arrhythmia, ischemic heart injury, and heart failure.[22–24] Experimentally, hypertrophied myocardium exhibit increased sensitivity to biochemical and metabolic changes during ischemia-reperfusion injury in the heart and decreased recovery of contractile function afterwards.[25,26] Pathological cardiac hypertrophy thus not only increases the susceptibility of the myocardium to ischemia-reperfusion injury but also augments the injurious response.[25]

Although there exist many molecular mechanisms that mediate myocardial hypertrophy, calcineurin–nuclear factor of activated T cells (NFAT) signaling is a well-characterized

pathway of significant interest.[27] Calcineurin is a calcium-dependent serine/threonine protease that can serve as a major pro-hypertrophic signaling molecule in the myocardium.[28] Physiologically, calcineurin associates with calcium-bound calmodulin; an elevated concentration of calcium therefore increases its enzymatic activity, dephosphorylating NFAT and inducing its nuclear translocation.[28,29] However, upon constitutive activation in mouse cardiomyocytes, calcineurin induces genetic, molecular, and phenotypic hallmarks of hypertrophied myocardium and heart failure, which are rescued both *in vivo* and *in vitro* by pharmacological calcineurin inhibition.[30] Considering that calcineurin-NFAT activation is shown to be both necessary and sufficient in the development of myocardial hypertrophy, it serves as an integral pathway to probe in investigations of cardiac remodeling.[31]

1.2.3 Fibrosis of the Heart

Pathological hypertrophy may also result from an increase in nonmyocytes within the heart via cardiac fibrosis. Endothelial cells and cardiomyocytes are the predominant cell types found in the normal heart, and fibroblasts constitute a marginal fraction of nonmyocytes.[32] Pathological stimuli, however, can induce myocardial fibrosis, which is defined by an increase in extracellular matrix within the heart.[21] Cardiac fibrosis not only increases the stiffness of the heart, which impedes contractility, but it also results in altered heart architecture and cardiac dysfunction. Currently, there are no molecular markers specific to cardiac fibroblasts, partially a result of their heterogeneous origins.[33] However, transforming growth factor beta (TGFβ) is a well-characterized mediator of cardiac fibrosis. Three isoforms of TGFβ (TGFβ I, II, and III) are found in mammals, and these generally bind to their respective receptor to activate the Smad2/3 pathway and promote fibrosis of the heart.[33] Specifically, the binding of TGFβ to the TGFβ type I receptor phosphorylates the

type II receptor, recruiting Smad 2 and Smad 3, which form a heterotrimer with Smad 4 to then translocate into the nucleus and regulate target genes; this increases the gene expression of extracellular matrix molecules, including collagen and fibronectin, promoting extracellular matrix deposition in the heart.[33] Cardiac fibrosis is particularly characteristic of an increase in the accumulation of both type I and type III collagen.[34,35] Once these pro-collagen chains are secreted from myofibroblasts within the heart, they are processed and assembled into fibrils, and then crosslinked; it is this crosslinked collagen that has been shown to be associated with both altered cardiac remodeling and cardiac dysfunction within the pathologically hypertrophied heart.[36–38] As such, type I and type III collagen serve as critical markers of pathological hypertrophy mediated by TGFβ activation and fibrosis.

1.2.4 Nitric Oxide Signaling in Cardiac Hypertrophy

NO is a signaling molecule that's primarily produced by endothelial NO synthase (eNOS), but also by inducible NOS (iNOS) and neuronal NOS (nNOS) isoforms in the heart.[39] Exercise is known to stimulate beta adrenergic receptors in endothelial cells, phosphorylating and activating eNOS to generate NO and promote vasodilation and angiogenesis in physiological hypertrophy.[40–42] As such, NO signaling adds a dimension of complexity to the pathological calcineurin-NFAT pathway. Pharmacological and genetic inhibition of eNOS-mediated NO generation in mice is shown to increase cardiomyocyte size and induce myocardial hypertrophy, fibrosis, and dysfunction, all of which are abrogated by restorative eNOS therapy.[43] Furthermore, overexpression of the gene encoding eNOS, *NOS3*, is shown to attenuate hypertrophy in addition to its cardioprotective effects against pressure overload.[43,44] Anti-hypertrophic effects of NO are shown to manifest by its cGMP-mediated activation of PKG, which suppresses NFAT transcriptional activities and inhibits the

molecular and phenotypic markers of hypertrophy in cardiomyocytes and myocardium.[45] Although PKG deletion neither potentiates nor alters the degree of hypertrophy compared to that induced by either pharmacological agent or surgical intervention, its negated role in hypertrophic development suggests that PKG has a limited role in hypertrophy upstream of its anti-hypertrophic effects by NFAT inhibition.[46] Altogether, interplay between the NO-cGMP and calcineurin-NFAT signaling pathways must be considered in an investigation of remodeling-induced alterations in the context of cardioprotection.

1.3 Myocardial Ischemia-Reperfusion Injury

Restoration of blood flow to the heart following a period of circulatory restriction/occlusion can induce ischemia-reperfusion (I/R) injury in the muscle tissue of the heart—the myocardium.[47] Ischemia, the first component of I/R injury, generates oxygen debt, which inhibits oxidative phosphorylation; this depletes adenosine triphosphate (ATP) and induces a cascade of biochemical and metabolic alterations with a shift towards anaerobic respiration that increases cytosolic calcium, decreases cardiomyocyte contractility and mitochondrial membrane permeability, and induces cell swelling and necrosis.[48,49] Reperfusion, though shown to reduce ischemic infarct size by 40% in animal models in part by reactivating the electron transport chain and restoring physiological pH, also has deleterious effects that are mediated by calcium and reactive oxygen species (ROS), resulting in ventricular arrhythmia, contractile dysfunction, microvascular obstruction, and/or lethal cardiomyocyte injury.[49–51] Cardioprotection against I/R injury refers to the reduction of these consequences and is shown to act endogenously *in vivo* among premenopausal females in part by estrogen and nitric oxide (NO) signaling pathways, which contribute to their decreased risk of CVD.[52–54] Considering that toxicity and biotransformation of environmental metals are also evidenced

to differ by sex, investigation of these toxicants' effects on sex-dependent cardioprotective signaling pathways is warranted.[55]

1.3.1 Nitric Oxide Signaling in Ischemic Heart Injury and Cardioprotection

NO widely regulates cardiovascular homeostasis and plays a critical role in reducing I/R injury.[54,56] *S*-nitrosylation (SNO), for example, is an NO-dependent post-translational modification that can shield thiol groups from oxidation and modulate a variety of proteins including estrogen receptors and calcium channels to confer cardioprotection.[56–59] Cyclic guanosine monophosphate (cGMP) is another ubiquitous intracellular second messenger that can be endogenously synthesized by the binding of NO with soluble guanylyl cyclase (sGC) in the cytosol.[60] Stimulation of NO production via eNOS increases cGMP production and activates protein kinase G (PKG), which has a number of targets that can modulate myocardial contractility.[61] NO-activated PKG can also activate protein kinase C, which is shown to open a mitochondrial ATP-dependent potassium channel that can consequently confer mitochondrial-mediated cardioprotection.[62,63] Separately, NO-activated cGMP can increase phosphodiesterase 2 activity, which inhibits protein kinase A, decreasing phospholamban and sarcoendoplasmic reticulum calcium ATPase activities; this increases calcium sequestration, decreases calcium cycling, and reduces cell death, promoting cardioprotection.[60] Altogether, the NO-cGMP signaling axis presents a pathway of particular interest in investigations of altered susceptibilities to I/R injury.

1.4 Environmental Exposures and Cardiovascular Disease

Despite advancements in its treatment and prevention, CVD remains the world's leading cause of death.[6,7] Environmental agents such as metals and air pollution are increasingly

implicated in CVD etiology and pathogenesis.[5,64] Air pollution, for example, has jumped to being the third leading risk factor for CVD mortality after extensive investigation into its effects on the cardiovascular system.[7,65,66] Considering the possibility that the prevalence and mortality of CVD continues to grow in spite of clinical management and intervention, it is possible that part of the challenge in preventing its escalation results from a fundamental gap in the understanding of the complex interplay between chronic environmental exposures and the cardiovascular system.[67]

1.4.1 Exposure to Inorganic Arsenic and Associated Cardiac Pathologies

Growing evidence highlights arsenic as a potential modifier of cardiovascular structure and function.[5] Arsenic is a naturally-occurring metalloid that enriches the earth's crust.[68] Leach into groundwater in addition to that accumulated from anthropogenic sources constitutes a majority of its presence in groundwater and foods such as rice and grains.[69] Human exposure to arsenic occurs predominantly via ingestion of contaminated drinking water, in which arsenic exists in an inorganic form (iAS) in either a trivalent or pentavalent oxidation state.[70,71] Following ingestion of contaminated drinking water, over 95% of the iAS is absorbed and then biotransformed into monomethylated (MMA) and dimethylated (DMA) metabolites, each associated with different health effects.[71] Ecological studies correlate iAS exposure among large populations in several countries with a dose-dependent increase in the risk and incidence for CVD.[72] Exposure to iAS is also epidemiologically and experimentally associated with other risk factors for CVD such as diabetes, abnormal electrocardiography, and hypertension. As(III) but not As(V) is shown to alter cardiovascular function by reducing the amount of blood pumped from the left ventricle in rat and rabbit models.[73] Beyond differential metabolite toxicology, long-term exposure to iAS is shown to increase

blood pressure, ventricular wall thickness, and left ventricular mass in female mice; this increase in blood pressure and heart size is also corroborated by cross-sectional studies in human populations.[74–76] Separately, iAS exposure is associated with a prolonged period of repolarization after each cardiac cycle in females but not in males as evaluated by electrocardiography (ECG) in a substantial prospective cohort study, highlighting certain sex-disparate effects at the population level.[77] Seeing as iAS exposure is also implicated in the reduction of NO levels by way of eNOS dysfunction, which may induce an array of alterations in cardiovascular physiology and signaling as described, an investigation into the effects of iAS on ischemic heart injury is justified.[78]

1.4.2 Inorganic Arsenic Exposure and Ischemic Heart Injury

Recent findings from this laboratory show that exposure to iAS at 1000 parts per billion (ppb or μg/L) for four weeks exacerbates I/R injury in female mouse hearts and attenuates injury in that of males (Fig. 1a, b).[79] Echocardiography also reveals myocardial enlargement in iAS-exposed female hearts (Fig. 1c).[79] Although iAS-exposed male hearts are not morphologically altered, they exhibit an increase in eNOS phosphorylation at serine-1177, an activating site of the cardioprotective enzyme (Fig. 1d).[79] Considering that the structural remodeling of female hearts manifested independently of eNOS phosphorylation or expression, these results suggest that iAS exposure induces sex-disparate effects and modulates susceptibility to IHD by targeting distinct sex-dependent pathways, laying ground for future studies to investigate the molecular mechanisms that underlie these effects.

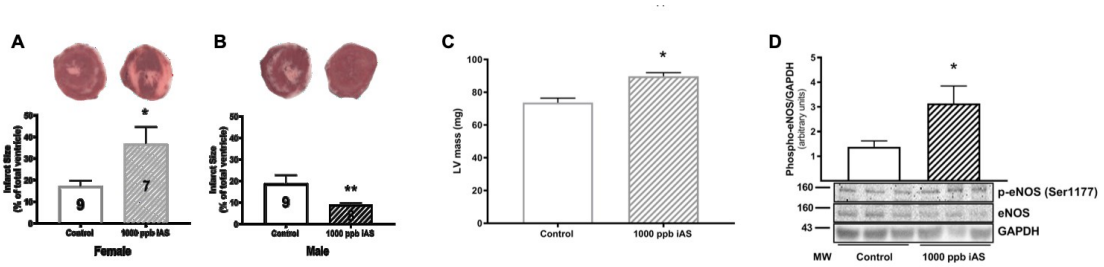

Figure 1. Summary of findings following a four-week, 1000 ppb iAS exposure in mice. Post-I/R infarct size **(a)** increases with exposure in female hearts but **(b)** decreases in males. **(c)** Left ventricular mass shows a modest increase with iAS in females. **(d)** Phosphorylation of eNOS at serine-1177, an activating site, is increased in males.

1.5 Specific Aims

Several studies provide evidence that myocardial I/R injury is increased by the male sex and attenuated by the female sex.[80–84] Veenema et al. highlight a reversal in this response following a four-week exposure to iAS via drinking water in mice.[79] However, epidemiological studies utilizing large, chronically-exposed populations across several countries do not corroborate an iAS-induced sex difference in the incidence of ischemic heart disease (IHD), suggesting that the observed cardioprotection is not maintained in the long-term.[85] Because modest sex-disparate effects manifested with a narrow window of exposure, an extension of the model is proposed to elucidate potential mechanisms through which iAS modulates susceptibility to I/R injury. We therefore hypothesized that an eight-week exposure to 1000 μg/L iAS induces cardiac remodeling and exacerbates myocardial I/R injury in both sexes.

1.5.1 Evaluate the impact of iAS exposure on I/R injury and cardioprotection

Mechanistically, it is possible that an increased phosphorylation of eNOS at four weeks of exposure in males led to an upregulation of the previously described cGMP-PKG signaling pathway, which is not only independently cardioprotective but also suppressive of cardiac hypertrophy. Because an iAS-induced reduction of hypertrophy or I/R injury is not observed at the epidemiological level, it is hypothesized that an extension of the exposure model abrogates cardioprotection and activates additional pathways inducing myocardial pathologies. Following the overarching hypothesis, it is expected that an eight-week iAS exposure will increase myocardial infarct size and decrease functional recovery of the heart following I/R in both sexes. Compared to pre-ischemic values, post-ischemic left ventricular developed pressure and rate pressure product are expected to decrease with iAS exposure. Additionally, infarct size is expected to increase with iAS exposure in both sexes.

Four-week exposure to iAS is shown to increase eNOS phosphorylation in males and not in females, which may lead to increased NO synthesis and promote subsequent attenuation of I/R injury early-on.[79] However, it is possible that this male cardioprotection is a quirk of utilizing an animal model that can better metabolize iAS for only a brief exposure period. An extended exposure to iAS is thus hypothesized to downregulate eNOS in both sexes and abrogate cardioprotection.

1.5.2 Define the implications of iAS exposure on remodeling of the myocardium

Results from a four-week exposure to 1000 μg/L iAS suggest modest cardiac enlargement in females. As such, it is also hypothesized that eight weeks of iAS exposure induces greater myocardial hypertrophy in both sexes, perhaps increasing susceptibility to I/R injury.

Hypertrophy of the heart is defined by altered cardiac structure and hemodynamics. Characterization of these properties will test the hypothesis that exposure to iAS increases blood pressure and induces cardiac remodeling. Exposure to iAS is expected to increase blood pressure and the heart weight to tibia length ratio. Additionally, histology is expected to reveal fibrosis in iAS-exposed hearts. Considering that calcineurin-NFAT signaling has a necessary and sufficient role in the development of cardiac hypertrophy, quantification of the expression and activity of this pathway will test the hypothesis that exposure to iAS upregulates calcineurin-NFAT signaling to promote pathological remodeling of the heart.

1.5.3 Overall study goals and significance

Ischemic heart disease (IHD) remains the world's leading cause of death.[86] Environmental agents such as metals and air pollution are increasingly implicated in the development of CVD, including IHD.[5] Although there exists a greater age-adjusted IHD mortality rate among males compared to that of premenopausal females, exposure to iAS via drinking water for four weeks is shown to reverse the expected, exacerbating ischemia-reperfusion (I/R) injury in the female mouse heart while lessening it in that of males.[79,87] Considering that these sex-disparate effects are not observed at the ecological level among chronically-exposed populations, the proposed study seeks to utilize an extended eight-week exposure to observe a hypothesized (Aim 1a) increase in susceptibility to myocardial I/R injury, (Aim 1b) downregulation of cardioprotective signaling pathways, (Aim 2a) increased cardiac remodeling, and (Aim 2b) upregulated hypertrophic signaling pathways in both sexes, thereby serving as a potential mechanism by which chronic exposure to iAS modulates susceptibility to ischemic heart injury.

Should phenotypic results indicate increased I/R injury and cardiac remodeling in males and females, this study may be the first to highlight that iAS exposure alters susceptibility to I/R injury by inducing cardiac remodeling. Additionally, this long-term exposure may illuminate molecular changes in NO signaling pathways that were previously unobserved due to a brief period of exposure. Regardless of whether data supporting the hypotheses are observed, results from the proposed experiments are essential to further define the effects of iAS exposure on the myocardium. Findings from this study will be useful in investigating sex-dependent mechanisms by which iAS promotes other CVD pathologies, which may, in the long-term, lead to the development of clinical and public health strategies to prevent the injurious effects of iAS on the cardiovascular system.

CHAPTER 2

INORGANIC ARSENIC INDUCES SEX-DISPARATE CARDIAC HYPERTORPHY

2.0 Introduction

Cardiovascular disease (CVD) remains the leading cause of death throughout the world.[6,7] Traditionally, risk factors for CVD have been considered personally modifiable such that the notions of increasing physical activity, avoiding tobacco smoke, and adhering to dietary approaches to stop hypertension are recommended to the general public.[88] However, growing evidence implicates environmental agents such as metals and air pollution in CVD etiology and pathogenesis.[5,64] Considering that the latter has jumped to the third leading risk factor in the global burden of disease, behind high blood pressure and tobacco smoke, the modulation of CVD and its risk factors by environmental agents must be studied.[7,65,66]

Arsenic is a naturally-occurring metalloid found in the Earth's crust that leeches into drinking water, which is the primary mode of human exposure.[71] The World Health Organization lists arsenic as one of ten chemicals of major public health concern, recommending a maximum limit of 10 μg/L in water supplies. However, the levels of arsenic in drinking water, existing as inorganic arsenic (iAS), have been found to exceed 1000 μg/L in some parts of the United States and 5000 μg/L in other parts of the world.[68,71] Chronic iAS exposure has been linked to several disease states, particularly diabetes, CVD, and cancer.[89,90] Although exposure to iAS is well-associated with adverse CV outcomes, the mechanisms through which it induces these health consequences are largely unknown.[91,92]

Previous findings from our laboratory showed that a four-week exposure to 1000 μg/L iAS was sufficient to exacerbate ischemic injury in female mouse hearts but not in males, highlighting sex-dependent cardiac remodeling as a potential mode of action.[79] Additionally, recent findings from the Strong Heart Study show that individuals exposed to iAS exhibit altered left ventricular geometry.[93] Considering that sex-disparate effects of iAS have not observed at the ecological level in chronically-exposed populations, we utilized an extended model of exposure in the current study to investigate the effects of iAS on myocardial structure and function in male and female hearts. We report for the first time that exposure to an environmentally relevant dose of iAS induces sex-dependent pathological hypertrophy of the heart, in part by upregulating the calcineurin-NFAT signaling pathway. As such, these findings confer mechanistic significance to the detrimental impact of iAS exposure on cardiovascular health, highlighting the need for its removal from human consumption.

2.1 Methods

2.1.1 Animals and Exposure Protocol

Seven-week-old male and female C57BL/6J wildtype mice (Jackson Laboratory, Bar, Harbor, ME) were housed (5 mice per cage) under pathogen-free conditions and maintained on AIN-93G chow (Research Diets, New Brunswick, NJ) and Nestle Pure Life water (Nestlé Waters North America, Stamford, CT) for one week prior to iAS exposure. Both the water and the chow are reported to have undetectable iAS levels, and the water was re-validated via inductively coupled plasma mass spectrometry (ICP-MS; Agilent 7500ce Octopole; Agilent Technologies, Santa Clara, CA) to have an iAS concentration less than its 0.16 μg/L limit of detection.[94,95] Following a one-week pre-exposure acclimation period, mice received water with 0 or 1000 μg/L sodium arsenite ($NaAsO_2$; S7400; Sigma-Aldrich, St. Louis, MO) *ad*

libitum for eight weeks; water and chow were refreshed every two to three days to minimize oxidation, and bedding was changed weekly. iAS exposure was further confirmed by the detection of iAS in urine samples via ICP-MS in exposed groups and the lack thereof in control groups (data not shown). Mice were anesthetized prior to subsequent procedures via intraperitoneal ketamine-xylazine injection (90 mg/kg ketamine, Hofspira, Lake Forest, IL; 10 mg/kg xylazine, Sigma Aldrich, St. Louis, MO), confirmed for adequacy via toe pinch. All animal work in this investigation conformed to the Guide for the Care and Use of Laboratory Animals published by the National Institutes of Health (NIH; Publication No. 85-23, Revised 2011) and was approved by the Institutional Animal Care and Use Committee of Johns Hopkins University.

2.1.2 Blood Pressure Measurement

Mice were acclimated to a tail-cuff pressure transduction apparatus (BP-2000 Blood Pressure Analysis System; Visitech Systems, Apex, NC) for one week prior to the onset of exposure and data collection in order to minimize systolic standard deviation and ensure reproducibility. Mice were restrained by opaque, open-bottomed rodent holders (BP-MH0; Visitech Systems, Apex, NC) that facilitated breathing and limited light exposure to calm the animal and reduce stress; the platform was preheated and maintained at 38°C in the dark under a laminar flow hood, and the tails were secured to the platform with surgical tape (3M Transpore Surgical Tape; 43149; 3M Company, Maplewood, MN) to minimize movement. Twenty experimental measurements were taken on each mouse each session, preceded by five preliminary measurements which allowed the animals to become accustomed to the tail cuff inflation and restraint. Briefly, the instrument reads and determines pulse through the tail, after which it starts inflating the cuff. Transmission photoplethysmography determines

blood pressure by analyzing the variation in light transmitted through the tail; during systole, vessels dilate and scatter light with each pressure wave, while the reverse occurs during diastole. As such, diastolic pressure was recorded when the cuff's pressure of occlusion caused the waveform amplitude (vessel dilation) to decrease, and systolic pressure was recorded when the occlusion pressure was sufficient to completely collapse the waveform, thus not causing any further dilation. Waveforms were monitored for appropriate amplitude during each of the twenty readings, and all values were averaged for each mouse each day, excluding outliers as categorized by a systolic pressure beyond 1.75 standard deviations from the mean. Measurements were taken at the same time twice a week throughout the duration of the exposure, as well as every day of the first, fourth, and eighth weeks.

2.1.3 Transthoracic Echocardiography

Transthoracic echocardiography was performed in conscious mice using a Vevo 2100 system with a 40-MHz linear transducer (FUJIFILM; VisualSonics, Toronto, ON, Canada) as described. M-mode echocardiogram was acquired from the short-axis view of the left ventricle at the level of the mid-papillary muscles and at a sweep speed of 200 mm/s. From this axis view of the left ventricle, the following cardiac parameters were measured: left ventricular anterior wall thickness at end diastole (LVAWd), left ventricle internal diameter at end diastole (LVIDd), and left ventricle posterior wall thickness at end diastole (LVPWd). Percent fractional shortening (FS), percent ejection fraction (EF), and left ventricular mass (LV mass) were extrapolated from these parameters as measures of cardiac contractility and left ventricular morphology; these indices were derived from the following equations: FS (%) = $[(\text{LVIDd} - \text{LVIDs})/\text{LVIDd}] \times 100$, EF (%) = $[(\text{LVId}^2 - \text{LVIDs}^2)/\text{LVIDd}^2] \times 100$; and LV mass (mg): $1.055\ [(\text{LVAWd} + \text{LVIDd} + \text{LVPWd})^3 - (\text{LVIDd})^3]$, where 1.055 is the

specific gravity of the myocardium. Volumes at end-systole (Vs) and end-diastole (Vd), stroke volume (SV), and EF were estimated using the Simpson's method and the two-chamber view of the heart on long axis as well as the short axis. All echocardiography values were simultaneously generated/calculated using the LV trace function (Vevo 2100 Software).

2.1.4 Inorganic Arsenic Measurement

Samples of iAS-solubilized water, control water, and urine from each mouse was taken at the six-week timepoint using hydrophobic sand (Labsand, Braintree Scientific, Braintree, MA) and stored (−80°C) until analysis. Water and urine samples were blinded and analyzed by an independent laboratory. Briefly, samples (50 µL) were diluted into HNO_3 (2%) and HCl (0.5%) solution. Calibration curves for arsenic were built using a standard solution (Multi-element Aqueous CRM, QC Standard 21; VHG Laboratories, Manchester, NH). Ten µg/L (vol/vol) of internal standard (CPI International, Santa Rosa, CA) was added to samples and calibration curves to control for potential drifts in the signal. Arsenic concentrations were then measured using inductively coupled plasma mass spectrometry (Agilent 7500ce Octopole inductively coupled plasma mass spectrometer, ICP-MS; Agilent Technologies, Santa Clara, CA). The limit of detection was 0.16 µg/L for arsenic. Samples with iAS concentrations below the limit of detection were substituted by the limit of detection divided by the square root of two. For quality control and assurance, 10% duplicates, 10% blanks, Seronorm Trace Elements Urine (Accurate, Westbury, NY), and replicate sample analysis at predetermined intervals were analyzed.

2.1.5 Langendorff Heart Perfusion

Hearts from mice anesthetized by intraperitoneal ketamine-xylazine injection were excised, cannulated onto a Langendorff apparatus, and perfused retrogradely with Krebs-Henseleit buffer bubbled with oxygen (95%) and carbon dioxide (5%) under constant pressure (100 cmH_2O) and temperature (37°C). Buffer consisted of, in mmol/L: NaCl (120), KCl (4.7), KH_2PO4 (1.2), $NaHCO_3$ (25), $MgSO_4$ (1.2), d-glucose (11), and $CaCl_2$ (1.75); pH 7.4; this reflected most physiological components of blood, including sodium, potassium, glucose, and calcium, which allowed the isolated heart to spontaneously beat with perfusion.[96] Hearts were subjected to either a five-minute perfusion, after which they were sectioned into two halves and snap-frozen under liquid nitrogen, or ischemia-reperfusion as follows.

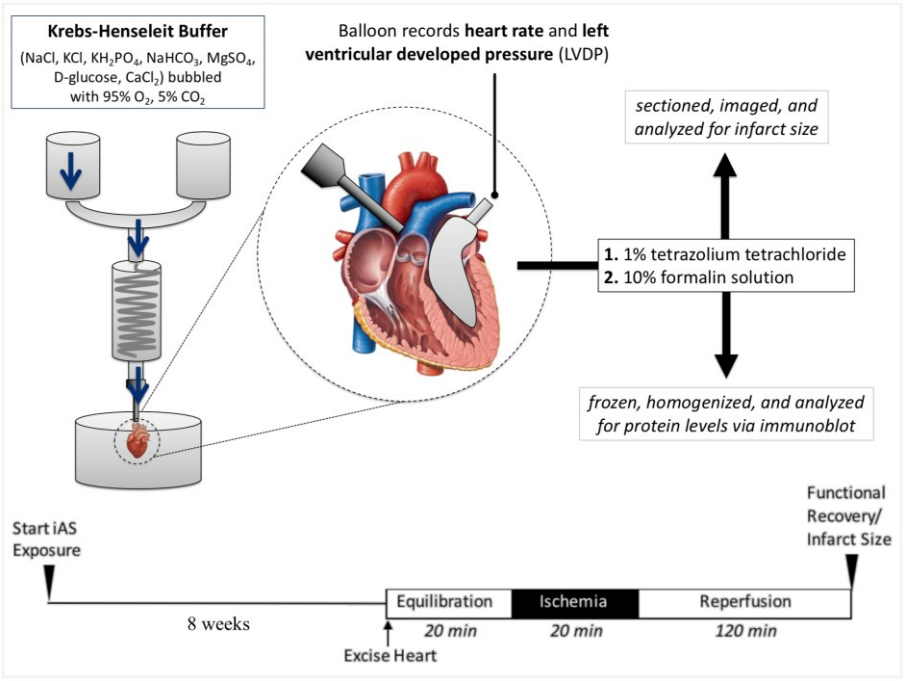

Figure 2. Overview of heart collection workflow. Hearts were perfused with Krebs-Henseleit buffer on a Langendorff apparatus. Hearts were then either subjected to I/R injury and stained for infarct analysis or snap frozen for molecular experiments.

2.1.6 Ischemia-Reperfusion Protocol

Immediately after Langendorff cannulation, a water-filled, saran-wrap balloon connected to a pressure transducer (PowerLab, AD Instruments, Dunedin, New Zealand) was inserted into the left ventricle of an excised heart to monitor and record digitized heart rate (HR) and left ventricular developed pressure (LVDP); rate pressure product (RPP) was calculated from these parameters and used as another metric of cardiac contractile function. Following a twenty-minute period of equilibration, perfusion was stopped for twenty minutes to induce global myocardial ischemia, and afterwards, the heart was re-perfused for two hours. Post-ischemic functional recovery and contractility at sixty minutes into reperfusion were expressed as a percentage of the pre-ischemic RPP and as a function of the change in LVDP over change in time (dP/dt), respectively. Following ischemia-reperfusion (I/R), hearts were perfused with triphenyltetrazolium chloride (TTC; 1%; 2 min), which is metabolized by intracellular dehydrogenases into a red pigment, staining viable cells and leaving the infarct white; hearts were then incubated (37°C, 20 min) in TTC solution and subsequently fixed in formalin solution (10%). Hearts were sectioned into five transverse parts, and the two sides of each section were imaged under a dissecting microscope (Nikon). Infarct size was analyzed by an investigator blinded to the treatment groups using ImageJ software (NIH, Bethesda, MD), quantifying infarcted myocardium as a function of total myocardial area in the section plane.

2.1.7 Histology

Sectioned, formalin-fixed hearts were paraffin-embedded and stained with either haemotoxylin and eosin (H&E) or Masson's trichrome to visualize cell morphology and fibrosis, respectively (Reference Histology Laboratory, Johns Hopkins Medical Institutions,

Baltimore, MD). Whole slides of Masson's-stained, paraffin-embedded hearts were scanned (20X, Aperio ScanScope) by a facility blinded to the treatment groups (Oncology Tissue Services, Johns Hopkins Medical Institutions, Baltimore, MD). Digital slides were subsequently analyzed (Aperio ImageScope) using a standard positive pixel count algorithm (Positive Pixel Count v9.1, Aperio, Leica Biosystems) according to the following parameters, set to read blue pixels as positive and red as negative, categorizing the former into three intensity bins: hue value = 0.62, hue width = 0.40, color saturation threshold = 0.04, intensity threshold (upper limit) of weak positive pixels = 220, intensity threshold (lower limit) of weak positive pixels = 175, intensity threshold (lower limit) of medium positive pixels = 100, intensity threshold (lower limit) of strong positive pixels = 0, intensity threshold of negative pixels = -1. Positivity, representing the number of positive pixels over the total number of positive and negative pixels, is reported as a quantification of myocardial collagen.

2.1.8 Plasma Enzyme Immunoassays

Blood was drawn from the inferior vena cava using a heparin-coated syringe and collected in a tube with heparin (10 μL) immediately after excision of the heart. Blood was centrifuged (21,130 x *g*, 10 min, 4°C), plasma was collected, and the samples were stored (-80°C) until use. Atrial natriuretic peptide (ANP) and B-type natriuretic peptide (BNP) were measured via enzyme immunoassay following manufacturer's instructions (EIA-ANP and EIA-BNP, RayBiotech, Norcross, GA).

2.1.9 Heart Homogenate Preparation

Hearts were homogenized with cell lysis buffer (1 mL, Cell Signaling Technology, Danvers, MA) supplemented with a protease-inhibitor cocktail (Cell Signaling Technology) in a hard tissue lysing kit (Precellys CK28 Lysing Kit, Bertin Instruments) under dry ice using a bead-mill tissue homogenizer (2 × 30 sec cycles, 0°C, 7200 RPM; Precellys Evolution 24, Bertin Instruments). Supernatant was recovered as total crude homogenate, protein concentration was determined via Bradford assay, and total homogenate aliquots were stored (-80°C).

2.1.10 Western Blot

Samples (30 μg) were separated on a graduated Bis-Tris SDS-PAGE gel (4-12%, NuPAGE, Invitrogen, Carlsbad, CA) and transferred to a nitrocellulose membrane (Life Technologies, Carlsbad, CA). Every gel included two molecular weight markers for separate regions of interest (High Range Color-Coded Prestained Protein Marker, Cell Signaling Technology; and Novex Prestained Protein Standard, Thermo Fisher Scientific, Rockford, IL). For normalization against total protein, lysine residues were covalently labeled (No-Stain Protein Labeling Reagent, Invitrogen) following manufacturer's instructions and visualized by fluorescence (Life Technologies). Membranes were blocked (1 hr) with bovine serum albumin (5% w/v; Sigma Aldrich) in tris-buffered saline with tween-20 (0.1%), and subsequently incubated (overnight, 4°C) with primary antibodies against p-Akt S473 (1:1000; 4060S, rabbit, Cell Signaling Technology, Danvers, MA), t-Akt (1:1000; 4691S, rabbit, Cell Signaling Technology), p-eNOS S1177 (1:500; 9570S, rabbit, Cell Signaling Technology), p-eNOS T495 (1:500; 9754S, rabbit, Cell Signaling Technology), t-eNOS (1:250; sc-376751, mouse, Santa Cruz Biotechnology, Dallas, TX), PKG-1 (1:1000; 3248S, rabbit, Cell Signaling Technology), p-VASP S239 (1:1000; 3132S, rabbit, Cell Signaling Technology), t-VASP

(1:1000; 3114S, rabbit, Cell Signaling Technology). Membranes were then probed (1 hr) with the corresponding secondary antibody, either anti-rabbit (7074S; Cell Signaling Technology) or anti-mouse (sc-2005; Santa Cruz Biotechnology), and visualized by electrogenerated chemiluminescence (Life Technologies). Membranes were stripped (Re-Blot Plus Mild Solution, EMD Millipore, Temecula, CA) and re-probed as needed. Densitometry was assessed using ImageJ software (NIH) and normalized to total protein.

2.1.11 RNA Isolation, Extraction, and cDNA Conversion

Hearts were homogenized with TRIzol (1 mL, Ambion) in a hard tissue lysing kit (Precellys CK28 Lysing Kit, Bertin Instruments) under dry ice using a bead-mill tissue homogenizer (2 × 30 sec cycles, 0°C, 7200 RPM; Precellys Evolution 24, Bertin Instruments). Chloroform (200 µL, Thermo Fisher) was added, and samples were subsequently shaken (30 sec), incubated (5 min, 25°C), and centrifuged (12,000 × g, 15 min, 4°C) for phase separation. RNA in the upper aqueous phase was carefully collected in a new centrifuge tube. Isopropyl alcohol (500 µL) was added, samples were incubated (10 min, 25°C), and centrifuged (12,000 × g, 8 min, 4°C) for RNA precipitation. After discarding the supernatant, the RNA pellet was washed with ethanol (500 µL, 75% EtOH), centrifuged (12,000 × g, 10 min, 4°C), and air dried under a laminar flow hood (30 min). RNA was solubilized (100 µL, DEPC-treated water), concentration and purity (A_{260}/A_{280} range 1.98 to 2.06) were obtained via spectrophotometry (1 mL sample, NanoDrop 100, Thermo Fisher), and integrity was confirmed via agarose (1%) gel electrophoresis (1X TBE (Tris base, boric acid and ethylenediaminetetraacetic acid (EDTA)) and 18S and 28S rRNA band visualization. RNA was subsequently converted to cDNA per manufacturer's instructions (4368814, High-Capacity cDNA Reverse Transcription Kit, Thermo Fisher). Briefly, the reverse transcription

reaction mix was prepared on ice, RNA (2 μg) was added, and the samples were run on a thermocycler (60 min, 37°C; 5 min, 95°C; held, 4°C; Applied Biosystems); cDNA was stored (-80°C) until use.

2.1.12 Quantitative PCR

Expression of mRNA transcripts was measured using a standard master mix (TaqMan Fast Advanced Master Mix) with the following validated probes (TaqMan, Applied Biosystems) on a thermocycler (2 min, 50°C; 2 min, 95°C; (1 sec, 95°C; 20 sec, 60°C) × 40), Applied Biosystems) in a 384-well plate: *Acta1* (Mm00808218_g1), *Akt1* (Mm01331626_m1), *Col1a2* (Mm00483888_m1), *Col3a1* (Mm00802300_m1), *Gapdh* (Mm99999915_g1), *Myh6* (Mm00440359_m1), *Myh7* (Mm00600555_m1), *Nppa* (Mm01255747_g1), *Nppb* (Mm01255770_g1), *Rcan1* (Mm01213406_m1). Expression was determined using the ΔΔCT method and normalized to *Gapdh*, which did not change with iAS treatment in either sex.

2.1.13 Electron Paramagnetic Resonance

Briefly, flash-frozen heart tissue (~20 mg) was homogenized in phosphate buffered saline (PBS) containing 0.1 mM diethylene-24 triaminepentaacetic acid (DTPA) and protease inhibitor cocktail (pH 7.4; Roche Applied Science, Indianapolis, IN). Non-soluble fractions were removed by centrifugation (15,000 x g, 10 min, 4°C), and the homogenates were kept on ice and analyzed immediately. Stock solutions of 1-hydroxy-3-methoxycarbonyl-2,2,5,5-tetramethylpyrrolidine hydrochloride (CMH; Enzo Life Sciences, Farmingdale, NY) were prepared daily in nitrogen purged 0.9% (w/v) NaCl, 25 g/L Chelex 100 (Bio-Rad) and DTPA (0.1 mM) and kept on ice; the samples were treated with CMH (1 mM, 37°C, 2 min), transferred to 50-μL glass capillary tubes, and analyzed on a Bruker E-Scan (Billerica, MA)

electron paramagnetic resonance (EPR) spectrometer at room temperature. Instrument settings were as follows: sweep width, 100 G; microwave frequency, 9.75 GHz; modulation amplitude, 1 G; conversion time, 5.12 ms; receiver gain, 2 x 10^3; number of scans, 16. EPR signal intensities were normalized with respect to the protein concentrations of the tissue homogenates as determined by Pierce BCA protein assay kit (Life Technologies).

2.1.14 Cell Culture Protocol

Human embryonic kidney 293 cells (HEK293, Invitrogen) were maintained (5% CO_2, 37°C, humidified air) in Dulbecco's Modified Eagle Medium (DMEM) with glucose (4.5 g/L) and L-glutamine (Gibco) supplemented with fetal bovine serum (10% FBS, Sigma-Aldrich) and 100 U/mL penicillin/100 μg/mL streptomycin (1% P/S, Gibco, Life Technologies).

2.1.15 Cell Proliferation Assay

HEK293 cells seeded in a 96-well plate (2×10^4 cells/well) were treated with sodium arsenite (0, 0.5, 1, 5, 10, 25, 50, and 100 μM in complete cell culture media, 37°C, 24hrs). MTT reagent (3-(4,5-dimethylthiazol-2-yl)-2,5-diphenyltetrazolium bromide; 50 μL/well; ab211091, Abcam) was then added and the cells were incubated (37°C, 1h). MTT solvent (150 μL/well; ab211091, Abcam) was added and the plate was shaken (orbital shaker, dark, 40 RPM, 10 min) to solubilize the formazan crystals; absorbance (590 nm) was promptly read. Cell proliferation is represented by optical density as a percent of the average control.

2.1.16 NFAT Luciferase Assay

HEK293 cells cultured in DMEM (10% FBS, 1% P/S, Thermo Fisher) to 70% confluence were transfected with plasmids expressing an NFAT-luciferase reporter (0.3 μg, Promega).

Plasmids expressing Renilla-luciferase (0.001 μg, Promega) and/or TRPC6 (0.2 μg) were transfected (Xfect Transcfection, Takara Bio USA, Mountain View, CA) as internal and positive controls, respectively. Transfected cells were exposed to sodium arsenite (0, 1, 5, 10 μM in complete cell culture media, 37°C, 24hrs). Cell lysate was then extracted using passive lysis buffer according to manufacturer's instructions (Promega), and luciferase activity measured by Dual-Luciferase Reporter Assay (Promega).

2.1.17 Statistical Analysis

Sample sizes of mice and cell culture for each experiment were estimated *a priori* via power analysis (power = 0.80, effect size = 0.25, $\alpha = 0.05$) based on data generated in previous studies from our group. Mice were also randomized during collection to minimize batch effects. Data were analyzed using GraphPad Prism (La Jolla, CA). Statistical outliers were identified by the ROUT method (Q = 1%). Statistical significance ($p < 0.05$) between groups was determined via two-tailed Mann Whitney test. All *p*-values are reported in their respective figure legend.

2.2 Results

2.2.1 Exposure to iAS does not change dietary intake or body weight

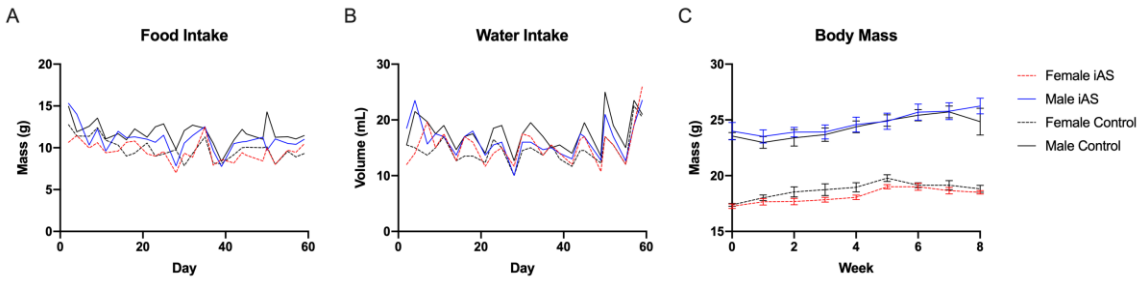

Figure 3. Dietary intake and body weight throughout an eight-week, 615 µg/L iAS exposure in mice. Exposure to iAS does not change **(a)** food intake, **(b)** water intake, or **(c)** body weight in male or female mice (n = 10 mice per group).

Food and water intake were monitored every two days throughout the duration of the exposure to ensure that cardiovascular pathologies, such as susceptibility to I/R injury, did not result from dietary restriction or dehydration.[97] No significant differences were observed in food intake, water intake, or body weight with iAS exposure in either sex (Fig. 3).

2.2.2 iAS induces sex-dependent increases in blood pressure and cardiac geometry

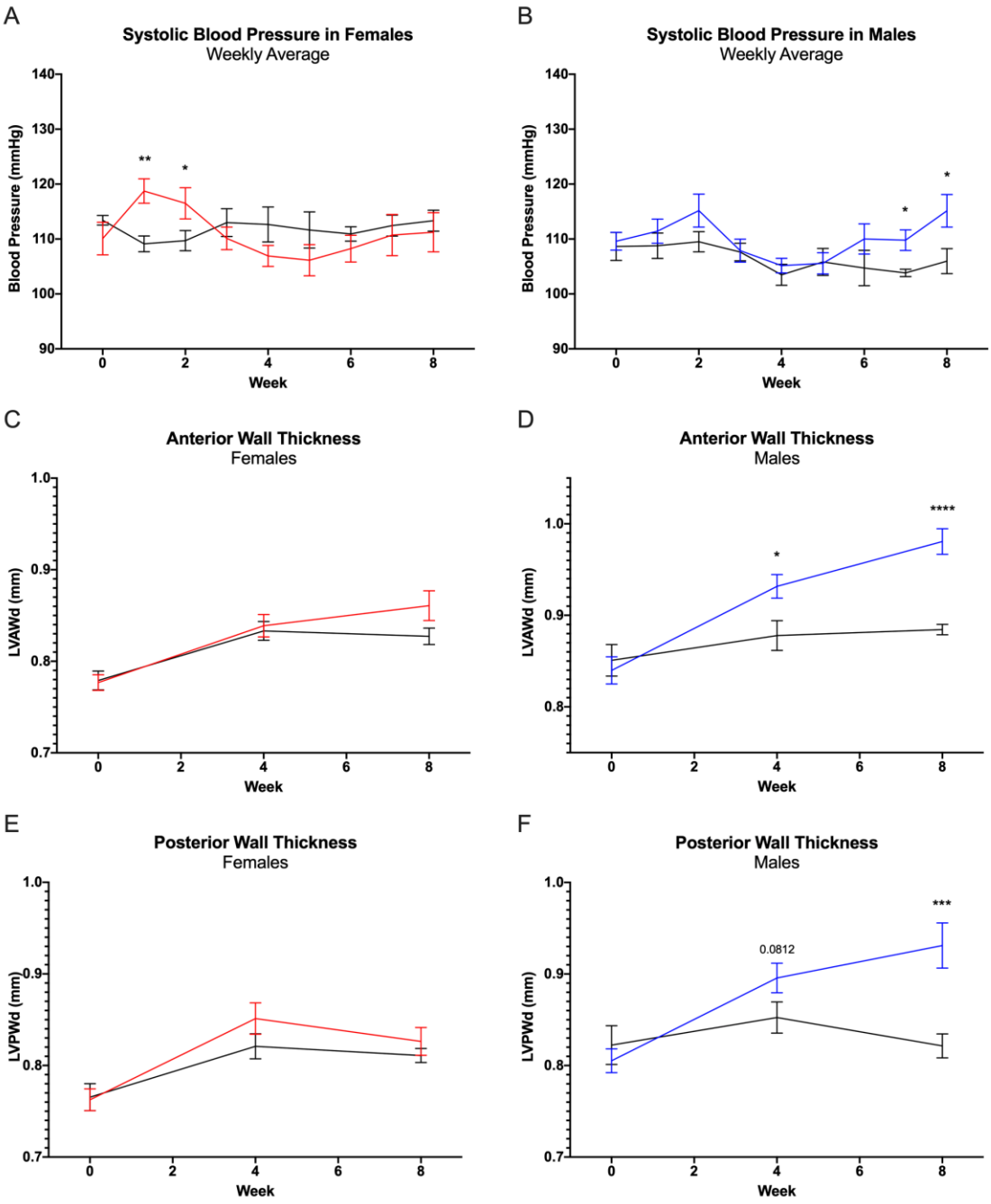

Figure 4. Exposure to iAS induces sex-dependent increases in systolic blood pressure and left ventricular wall thickness. Systolic blood pressure **(a)** in females increases during the first (difference = 9.253 mmHg, p = **0.0029) and second (difference = 4.110 mmHg, *p =

0.0433) weeks of exposure, but subsequently returns to baseline. Systolic blood pressure **(b)** in males increases during the seventh (difference = 6.082 mmHg, *p = 0.0434) and eighth (difference = 9.207 mmHg, *p = 0.0350) weeks of exposure. Left ventricular anterior wall thickness in diastole (LVAWd) **(c)** in females does not change at weeks zero, four, or eight. However, LVAWd **(d)** in males increases at weeks four (*p = 0.0172) and eight (****p < 0.0001). Left ventricular posterior wall thickness in diastole (LVPWd) **(e)** in females does not change at weeks zero, four, or eight. LVPWd **(f)** in males exhibits a trending increase at week four (p = 0.0812) and a significant increase at week eight (***p = 0.0002). Significance was determined by Mann Whitney test (n = 9 to 10 mice per group).

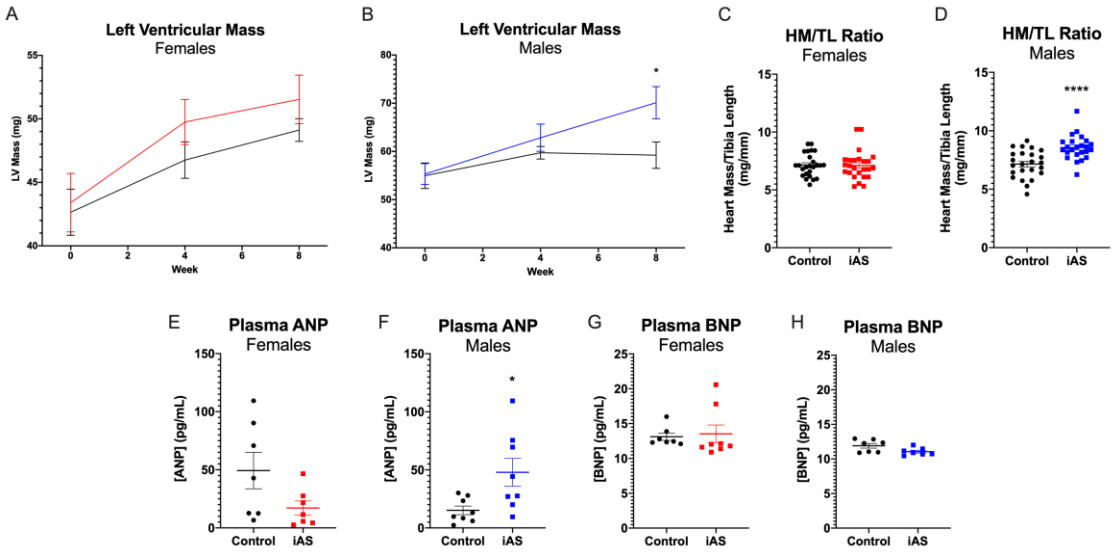

Figure 5. Exposure to iAS induces sex-dependent hypertrophy of the heart. Left ventricular mass (LV mass) extrapolated from transthoracic echocardiography **(a)** in females does not change at weeks zero, four, or eight. LV mass (n = 10 mice per group), but **(b)** in males increases at the eighth week of exposure (difference = 12.58 mg, *p = 0.0350; n = 9 to 10 mice per group). Heart mass normalized to tibia length (HM/TL) **(c)** in females does not change (n = 25 hearts per group), but **(d)** in males increases (****p < 0.0001; n = 24 to 25

hearts per group). Plasma atrial natriuretic peptide (ANP) **(e)** does not change in females (n = 10 mice per group), but **(f)** increases in males (*p = 0.0379; n = 9 to 10 mice per group). Plasma brain natriuretic peptide (BNP) does not change in either **(g)** females (n = 10 mice per group) or **(h)** males (n = 9 to 10 mice per group). Outliers were determined by the ROUT method (Q = 1%) and significance was determined by Mann Whitney test.

We previously reported that a four-week exposure to 1000 μg/L of iAS was sufficient to exacerbate myocardial I/R injury in females, but not in males. Furthermore, we found that interventricular septal wall thickness was increased in female hearts at the four-week endpoint. Considering the possibility that iAS imparts sex-disparate effects on the structure and function of the heart, and that these effects change over an extended model of exposure, transthoracic echocardiography was conducted at zero, four, and eight weeks of iAS exposure (measured to be 614.6 μg/L in the current study), and blood pressure was recorded throughout. Systolic blood pressure was significantly increased in iAS-exposed females during the first and second weeks of exposure (+9.617 and +6.810 mmHg, respectively), but subsequently regressed back to baseline (Fig. 4a). Systolic blood pressure in iAS-exposed males, however, significantly increased at the seventh and eighth weeks of exposure (+5.962 and +9.162 mmHg, respectively) (Fig. 4b). Consistent with this increase in systolic blood pressure in iAS-exposed males, we also found that anterior and posterior wall thickness was increased at eight weeks of exposure (Figs. 4d, f). Echocardiographic parameters in females, however, did not significantly change at either four or eight weeks of exposure (Figs. 4c, e). Additionally, left ventricular mass extrapolated from echocardiography showed an increase at the eight-week endpoint in males but not in females (Figs. 5a, b). As such, additional markers of a hypertrophic phenotype were probed. Heart weight normalized to tibia length was significantly increased in males but not in females (Figs. 5c, d), as were plasma ANP levels

(Figs. 5e, f). Although plasma BNP levels did not change in either sex (Figs. 5g, h), these data, taken together, indicate that exposure to iAS induces sex-dependent hypertrophy of the heart.

2.2.3 Exposure to iAS does not alter susceptibility to ischemic heart injury

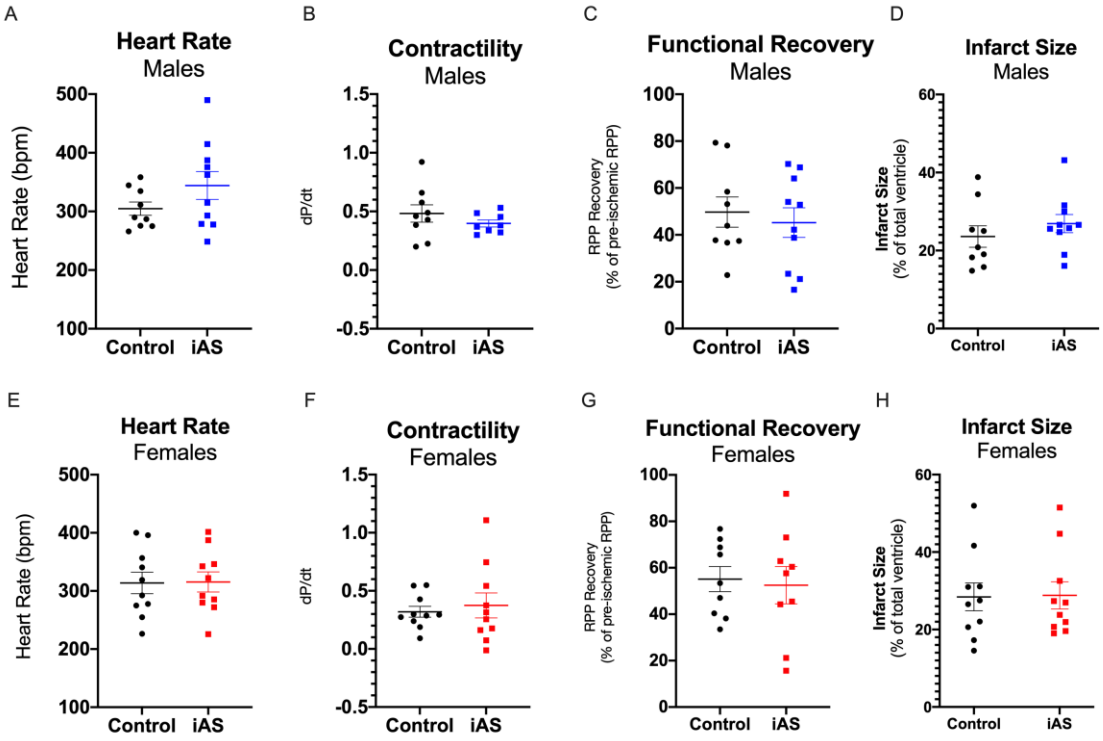

Figure 6. Exposure to 615 µg/L iAS for eight weeks does not alter susceptibility to ischemic heart injury. Langendorff-cannulated male and female hearts did not show changes in **(a, e)** baseline heart rate, **(b, f)** baseline contractility, quantified by a change in left ventricular developed pressure as a function of change in time (dP/dt), **(c, g)** post-ischemic functional recovery at 60 minutes into perfusion, and **(d, h)** post-I/R myocardial infarct size (n = 10 hearts per group).

To determine whether iAS-induced hypertrophy consequently altered myocardial ischemic susceptibility, several hemodynamic parameters were examined using an *ex vivo* model of I/R injury. Cardiac remodeling is an independent risk factor for adverse CV outcomes, and chronic iAS exposure has been particularly well-associated with ischemic heart disease.[98–103,92,72] Furthermore, a previous study from our group highlighted increased I/R injury in remodeled female hearts after a 1000 μg/L iAS exposure for four weeks.[79] As such, it was hypothesized that cardiac hypertrophy would increase I/R injury. Male and female hearts were thus subjected to I/R injury via Langendorff perfusion after the eight-week exposure period. Hemodynamic measurements indicated no differences in baseline heart rate, left ventricular developed pressure, and rate pressure product between iAS-treated and control male or female hearts (data not shown). Additionally, contractility, functional recovery, and infarct size did not change with iAS exposure in either sex (Fig. 6). As such, an eight-week iAS exposure does not appear to alter myocardial susceptibility to I/R injury.

2.2.4 iAS does not induce physiological hypertrophy or cardiac fibrosis

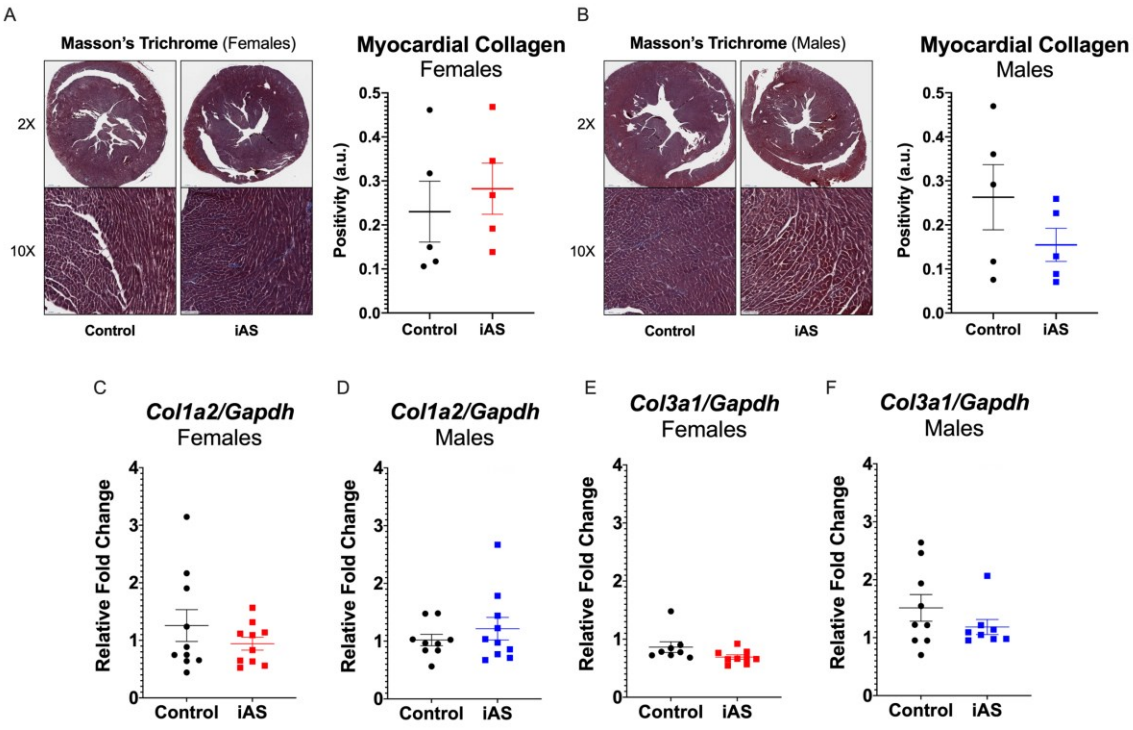

Figure 7. Exposure to iAS does not induce cardiac fibrosis. Masson's Trichrome histology does not reveal changes in collagen deposition in either **(a)** females (n = 10 hearts per group) or **(b)** males (n = 9 to 10 hearts per group). Myocardial mRNA transcript levels of collagen type I alpha 2 chain (*Col1a2*) did not change in either **(c)** females or **(d)** males. Myocardial mRNA transcript levels of collagen type III alpha 1 (*Col3a1*) also did not change in either **(e)** females or **(f)** males (n = 10 hearts per group). Transcript levels of each target were normalized to *Gapdh* mRNA expression, which did not change with iAS exposure in either sex. Outliers were determined by the ROUT method (Q = 1%) and significance was determined by Mann Whitney test.

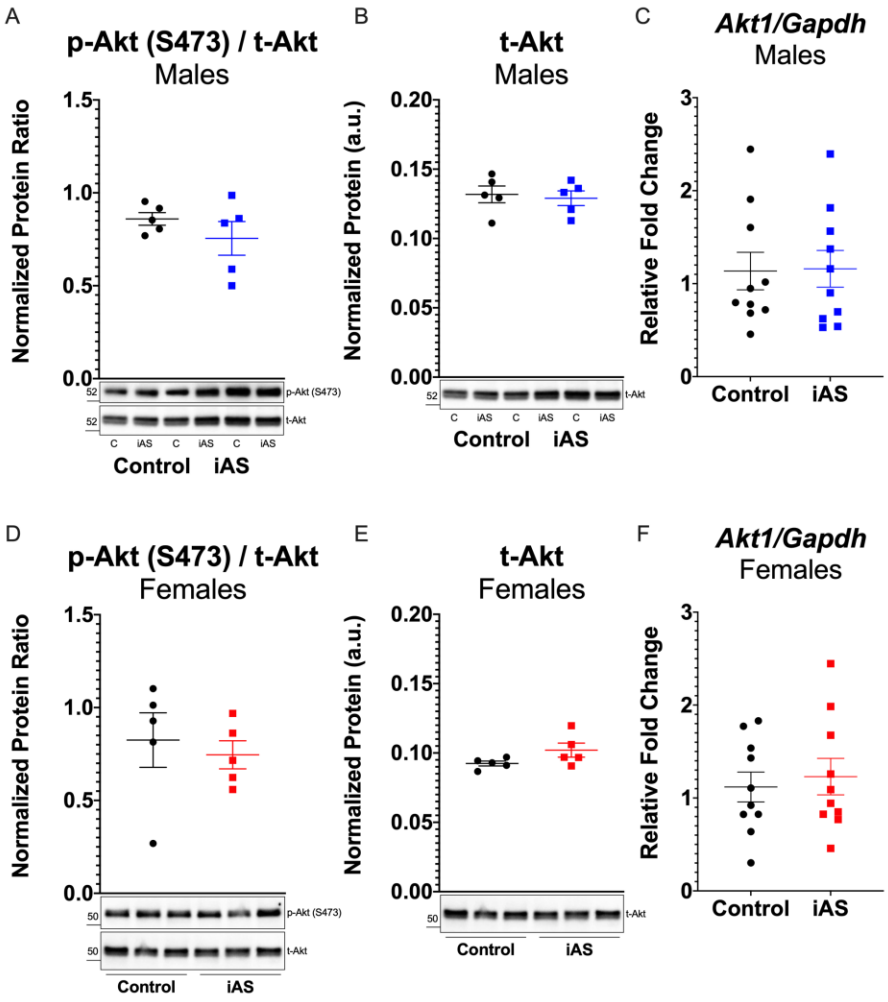

Figure 8. Exposure to iAS does not induce physiological hypertrophy in the heart. Protein expression of phosphorylated Akt (p-Akt) at serine 473 normalized to total Akt protein levels did not change in the **(a)** male and **(d)** female heart (n = 5 hearts per group). Protein levels of t-Akt did not change in the **(b)** male and **(e)** female heart (n = 5 hearts per group). Myocardial mRNA transcript levels of *Akt1* did not change in **(c)** males or **(f)** females (n = 10 hearts per group). Protein levels of each target were normalized to total transferred protein levels. Transcript levels of each target were normalized to *Gapdh* mRNA expression, which did not change with iAS exposure in either sex.

Because several studies have shown that iAS activates the TGF-β/Smad pathway and induces fibrosis in mice and rats, this investigation probed the possibility that the hypertrophic phenotype is driven by myocardial fibrosis.[104] Masson's Trichrome staining for collagen deposition, however, did not reveal an increase in fibrosis with iAS exposure in either sex (Figs. 7a, b). Additionally, this was confirmed by measuring mRNA expression of pro-fibrogenic extracellular matrix genes *Col1a2* and *Col3a1*, for type I and type III collagen, respectively, which showed no significant changes (Figs. 7c – f). Since there was no evidence that the phenotype was driven by myocardial fibrosis, the possibility that iAS induces physiological hypertrophy of the heart was probed. Akt is downstream of several signaling pathways known to facilitate developmental growth of the myocardium, and as such, Akt phosphorylation levels at serine 473, an activating site, total Akt protein levels, and Akt RNA transcript levels were probed in male and female hearts (Fig. 8). However, there were no significant changes in either sex, indicating that an eight-week exposure to 615 μg/L iAS is unlikely to induce either physiological growth or fibrosis of the heart.

2.2.5 Exposure to iAS induces pathological hypertrophy in the male heart

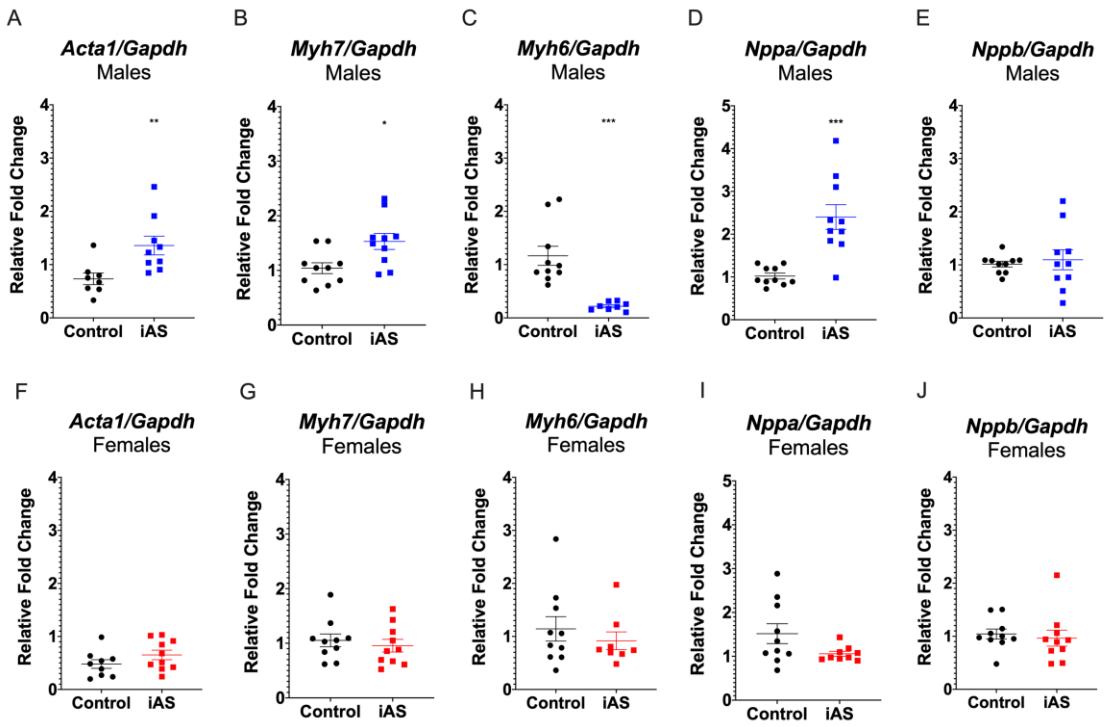

Figure 9. Exposure to iAS induces markers of pathological hypertrophy in the heart. Myocardial mRNA transcript levels of **(a)** skeletal muscle alpha-actin (*Acta1*) increases (**p = 0.0037), **(b)** beta myosin heavy chain (*Myh7*) increases (*p = 0.0138), **(c)** alpha myosin heavy chain (*Myh6*) decreases (***p = 0.0001), **(d)** natriuretic peptide A (*Nppa*) increases (***p = 0.0001), and **(e)** natriuretic peptide B (*Nppb*) does not change in males. However, mRNA expression of **(f)** *Acta1*, **(g)** *Myh7*, **(h)** *Myh6*, **(i)** *Nppa*, and **(j)** *Nppb* does not change in female hearts. Transcript levels of each target were normalized to *Gapdh* mRNA expression, which did not change with iAS exposure in either sex. Outliers were determined by the ROUT method (Q = 1%) and significance was determined by Mann Whitney test (n = 10 hearts per group).

Determination of whether iAS induces maladaptive growth of the myocardium was achieved by probing for downstream transcriptional markers of pathological hypertrophy. RT-qPCR revealed that mRNA expression of several genes coupled to pathological hypertrophy were increased with iAS exposure in males and not in females. Skeletal muscle alpha-actin (*Acta1*) and beta myosin heavy chain (*Myh7*) transcript levels exhibited an increase with exposure in males and not in females (Figs. 9a, b, f, g), and alpha myosin heavy chain (*Myh6*) showed a decrease in males and not in females, indicating an isoform switch (Figs. 9c, h). Additionally, natriuretic peptide A (*Nppa*) mRNA was significantly increased in males and not in females, while no change was observed in natriuretic peptide B (*Nppb*) transcript (Figs. 9d, e, i, j), consistent with levels of plasma ANP and BNP, respectively (Figs. 5e – h).

2.2.6 Further exposure to iAS may cause female hearts to lose protection

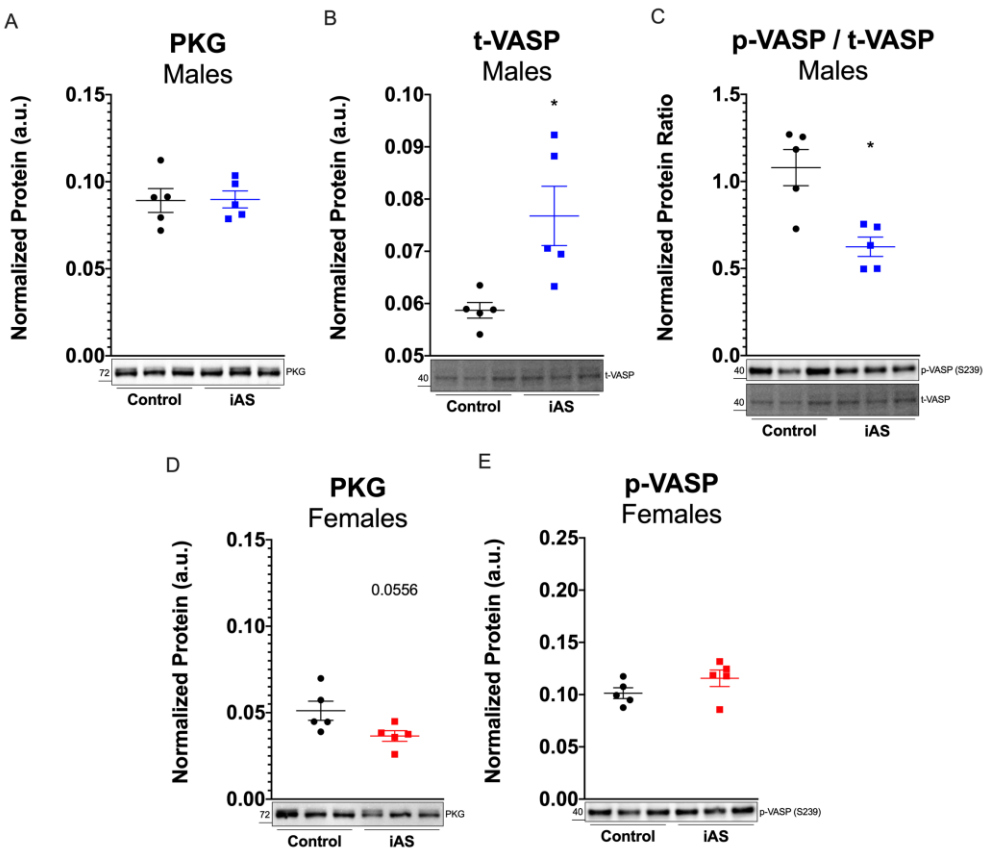

Figure 10. Exposure to iAS may alter PKG signaling in the heart. Male hearts exhibited **(a)** no changes in PKG protein expression, **(b)** increased protein expression of total vasodilator-stimulated phosphoprotein (t-VASP) (*p = 0.0159), and **(c)** decreased protein expression of phosphorylated VASP (p-VASP) at serine 239, a PKG site, normalized to t-VASP (*p = 0.0317). Female hearts exhibited **(d)** a decrease in PKG protein expression near significance (p = 0.0556), and **(e)** no changes in p-VASP. Protein levels of each target were normalized to total transferred protein levels. Outliers were determined by the ROUT method (Q = 1%) and significance was determined by Mann Whitney test (n = 5 hearts per group).

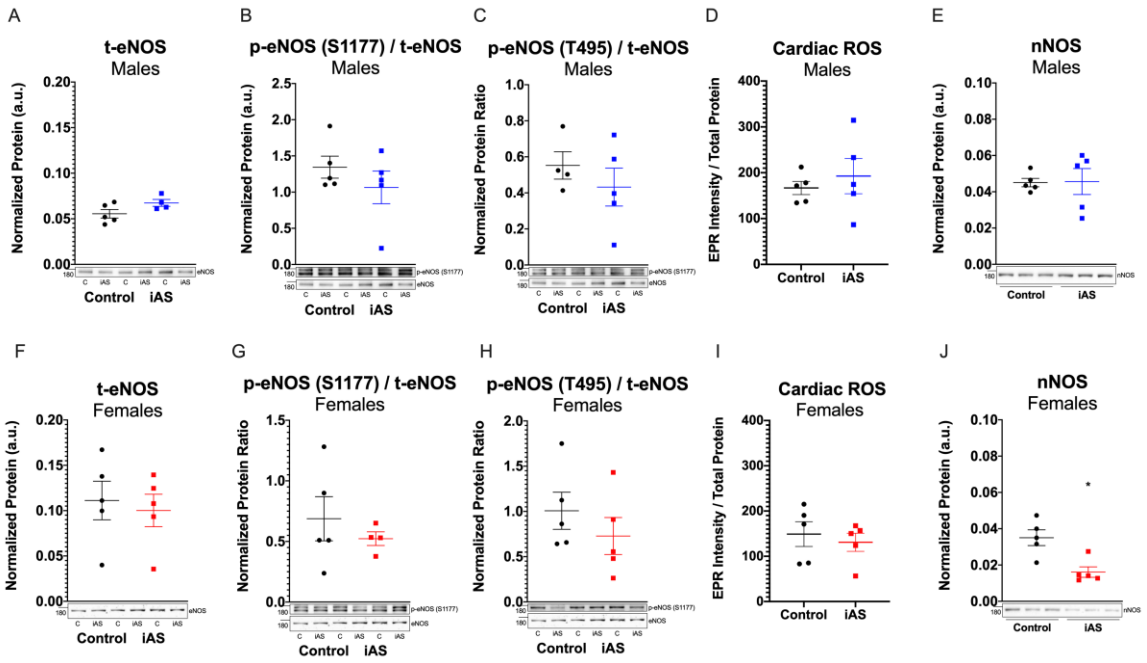

Figure 11. Exposure to iAS does not alter NO signaling in the heart. Male hearts exhibited no changes in **(a)** protein levels of total endothelial nitic oxide synthase (t-eNOS), **(b)** protein levels of phosphorylated eNOS at serine 1177, an activating site, (p-eNOS) normalized to t-eNOS, **(c)** protein levels of p-eNOS at threonine 495, an inhibitory site, normalized to t-eNOS, **(d)** cardiac reactive oxygen species (ROS) levels, and **(e)** protein levels of neuronal NOS (nNOS). Female hearts also did not exhibit any changes in **(f)** t-eNOS, **(g)** p-eNOS (S1177) / t-eNOS, **(h)** p-eNOS (T495) / t-eNOS, or **(i)** cardiac ROS, but **(j)** nNOS protein levels were decreased (*p = 0.0159). Protein levels of each target were normalized to total transferred protein levels. Outliers were determined by the ROUT method (Q = 1%) and significance was determined by Mann Whitney test (n = 5 hearts per group).

Since females did not demonstrate a hypertrophic phenotype following an eight-week iAS exposure, potential mechanisms underlying the observed protection were investigated. Western blot for total PKG expression, a mediator of cardioprotection, showed no

difference with iAS in males, but there was a significant decrease in females, suggesting a potential root to an eventual pathology in females (Figs. 10a, d). Protein levels of vasodilator stimulated protein (VASP) were significantly increased in males with iAS exposure (Fig. 10b), in accordance with the increase in systolic blood pressure, and protein levels of phosphorylated VASP at serine 239, a PKG site, were decreased in males but not in females, suggesting that PKG signaling may be impaired in males as part of the mechanisms leading to cardiac remodeling (Figs. 10c, e). Additionally, it was hypothesized that endothelial nitric oxide synthase (eNOS) may be upregulated in females and either downregulated or uncoupled in males, thus modulating the sex-dependent hypertrophic response. However, western blots for total eNOS, phosphorylated eNOS at serine 1177, an activating site, and phosphorylated eNOS at threonine 495, an inhibitory site, did not reveal significant changes with iAS exposure in either sex (Figs. 11a, b, c, f, g, h). Total iNOS protein levels were also probed but bands were not detected (data not shown). Myocardial superoxide levels were measured as a marker of eNOS uncoupling in heart homogenate via EPR, but iAS did not induce a change in superoxide production in either sex (Figs. 11d, i). Although protein levels of total nNOS were unchanged in iAS-exposed males, these levels were significantly decreased in iAS-exposed females (Figs. 11e, j). Seeing as the protein levels of both PKG and nNOS were significantly decreased in the female heart, these data suggest the potential for future pathology in females exposed to 615 μg/L iAS beyond eight weeks.

2.2.7 iAS activates NFAT independent of blood pressure

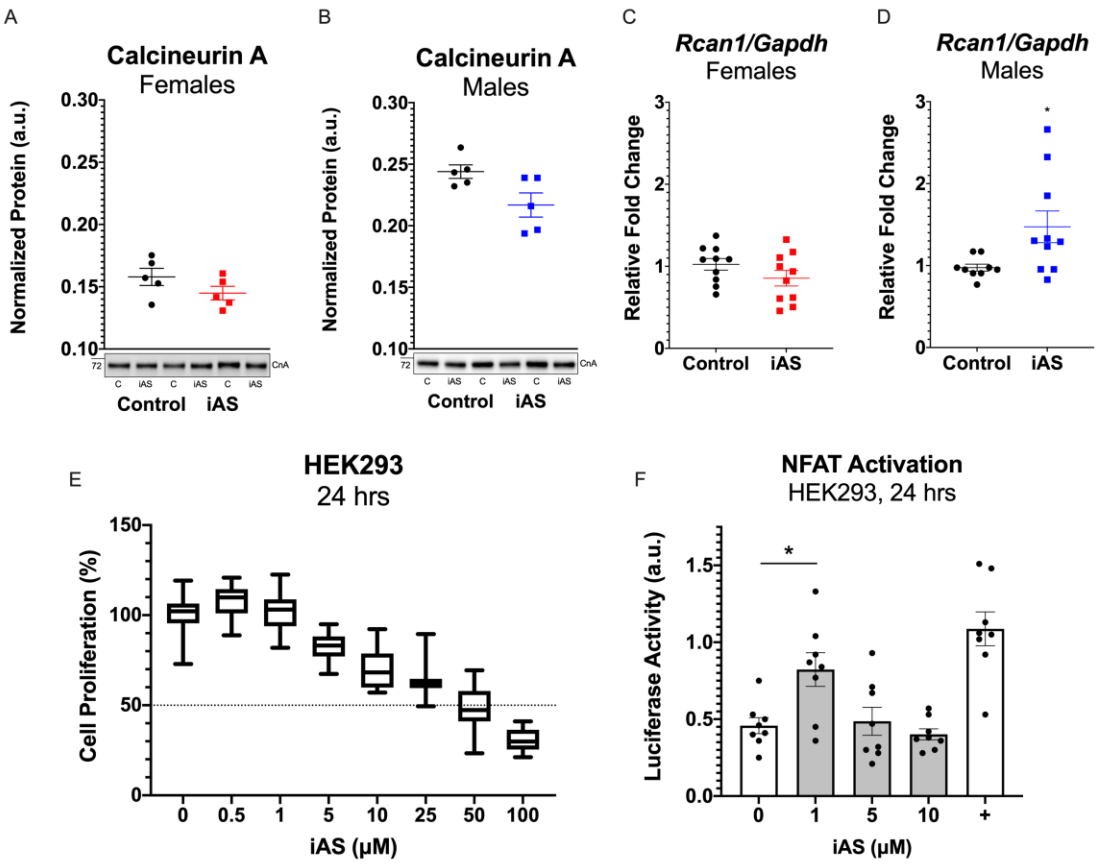

Figure 12. Exposure to iAS may activate the calcineurin-NFAT signaling pathway. Protein expression of calcineurin A were unchanged in **(a)** male and **(b)** female hearts (n = 5 hearts per group). Myocardial mRNA transcript levels of regulator of calcineurin 1 (*Rcan1*) were **(c)** unchanged in females, but **(d)** increased in males (*p = 0.0161) (n = 10 hearts per group). HEK293 cells treated with varying levels of iAS for 24 hours demonstrate **(e)** cell proliferation, represented by optical density as a percent of the average control, following a dose-response curve (n = 12 wells per group). HEK293 cells transfected with NFAT-luciferase and Renilla-luciferase, as well as *Trpc6* for a positive control (+), exhibited **(f)** increased NFAT-luciferase activity with a 1 μM iAS treatment for 24 hours (*p = 0.0214, n

= 8 wells per group). Protein levels of each target were normalized to total transferred protein levels. Transcript levels of each target were normalized to *Gapdh* mRNA expression, which did not change with iAS exposure in either sex. NFAT firefly luminescence was normalized to Renilla luminescence. Outliers were determined by the ROUT method (Q = 1%) and significance was determined by Mann Whitney test.

Considering that the calcineurin-NFAT signaling pathway is known to be upregulated with pathological and not physiological cardiac hypertrophy, total Calcineurin A protein levels in the heart were measured as a crude surrogate for calcineurin-NFAT activation, but these levels did not change with exposure in either sex (Figs. 12a, b). RT-qPCR, however, revealed that mRNA expression of regulator of calcineurin 1 (*Rcan1*), an NFAT target, was upregulated in iAS-exposed males and not in females (Figs. 12c, d), suggesting iAS may induce pathological hypertrophy of the heart in part by activation of calcineurin-NFAT. Taking blood pressure and echocardiography data into account, which characterized a significant increase in anterior and posterior wall thickness in males at four weeks of exposure prior to the observed increase in systolic blood pressure at weeks seven and eight, an *in vitro* exposure model was established to determine whether iAS can activate NFAT and induce hypertrophy independent of input from blood pressure. HEK293 cells were treated with varying concentrations of iAS for 24 hours, and an MTT cell proliferation assay revealed a dose-response curve with 50 μM iAS generating half-maximal proliferation (Fig. 12e). HEK293 cells transfected with an NFAT-luciferase reporter showed that NFAT luciferase activity significantly increased with a 1 μM iAS treatment for 24 hours, indicating that iAS directly induces the activation of NFAT, independent from blood pressure, as hypothesized (Fig. 12f). Together, these data suggest that iAS may activate calcineurin-NFAT signaling to promote pathological hypertrophy in the male heart.

2.3 Discussion

Epidemiological studies have associated chronic iAS exposure with the development of cardiovascular disease, and recent findings highlight an association with altered left ventricular geometry.[103,91–93] Herein, we find that exposure to an environmentally relevant dose of iAS through drinking water induces pathological hypertrophy of the heart in male mice but not females. We also report for the first time that iAS may induce these changes independent of blood pressure and fibrosis, in part by activating the calcineurin-NFAT signaling pathway.

Several epidemiological studies highlight an association between iAS exposure and both an increased systolic blood pressure in both biological sexes and an increased prevalence ratio for hypertension.[75,76,105–109] Experimental studies corroborate this increase in systolic blood pressure in both male rats exposed to 50 mg/L iAS for 28 weeks, and female mice exposed to 100 μg/L iAS for 22 weeks.[74,110] However, mechanistic studies also find that the effect of a chronic, low-level iAS on blood pressure often differs from that of higher levels.[104] Here, systolic blood pressure was significantly increased in female mice exposed to 615 μg/L iAS, measured to be 615 μg/L via ICP-MS, during the first and second weeks of exposure, but this increase returned to baseline through the eighth week (Fig. 4a). Considering that a previous study has reported an increase in systolic blood pressure in female mice following a longer exposure, and that iAS is not reported to induce a sex-disparate phenotype in the CV system at the epidemiological level, systolic blood pressure between iAS-treated and control female mice is expected to diverge with an extended model of exposure. Systolic blood pressure in males, on the other hand, increased at the seventh and eighth weeks of exposure (Fig. 4b). Additionally, anterior and posterior wall thicknesses of the left ventricle in males

increased with iAS exposure as measured at the eighth week, altogether demonstrating that iAS exposure induces cardiac remodeling (Figs. 4d, f).

Further examination of biological markers substantiated an iAS-induced hypertrophic phenotype in males and not in females. Left ventricular mass extrapolated from echocardiography increased with iAS in males at the eighth week, yet there was no change with iAS in females (Figs. 5a, b); this was confirmed by heart mass normalized to tibial length (Figs. 5c, d).[111] Plasma levels of atrial natriuretic peptide (ANP), which is stimulated by mechanical stretch of the atrial wall and is upregulated in cardiac hypertrophy, were increased in iAS-exposed males and not in females (Figs. 5e, f).[112] Plasma levels of B-type natriuretic peptide (BNP), however, which is also upregulated under hypertrophy, did not change with iAS exposure in either sex (Figs. 5g, h).[113] While ANP and BNP both promote anti-hypertrophic actions, the former primarily regulates cardiomyocyte size and blood pressure/volume, and the latter regulates cardiac fibrosis, in part by inhibiting the transforming growth factor-β (TGF-β) signaling pathway.[114–117] Quantification of myocardial collagen by image analysis showed no difference in cardiac fibrosis with iAS exposure in either sex, in accordance with plasma BNP levels (Figs. 3a, b). Additionally, measurement of *Col1a2* and *Col3a1* mRNA in the myocardium confirmed that iAS exposure did not upregulate TGF-β-responsive extracurricular matrix genes to induce cardiac fibrosis (Figs. 7c – f).[118,119] Although experimental literature has well-characterized that iAS can activate the TGF-β pathway to induce the fibrosis of several organs, including the heart, liver, and lung, these studies used significantly greater concentrations than that used in the current study.[104] We therefore probed previously uninvestigated mechanisms through which a chronic, low-dose, environmentally-relevant iAS exposure may induce cardiac hypertrophy.

Both physiological and pathological biomarkers were probed, revealing that iAS induces pathological hypertrophy of the heart. Epidemiological evidence does not suggest that iAS confers CV benefits, but echocardiography-derived ejection fraction, fractional shortening, and cardiac output did not change at this eight-week timepoint (data not shown).[79] As such, the possibility of physiological growth was examined. Akt is a downstream regulator of several critical processes involved in adaptive hypertrophy, including cell proliferation, growth, metabolism, and survival, and many studies have shown that iAS activates Akt through a variety of mechanisms in the context of carcinogenesis.[21,120–126] Levels of phosphorylated Akt protein at serine 473, an activating site, total Akt protein, and Akt mRNA were thus measured in the myocardium. However, these levels did not change with iAS exposure in either sex, suggesting that iAS exposure does not induce physiological growth of the heart (Fig. 8). Myocardial expression of a suite of genes upregulated in pathological hypertrophy was subsequently examined. Skeletal muscle alpha-actin, *Acta1*, increases in the hypertrophied heart and is associated with cardiac dysfunction.[127–129] RNA sequencing data also reveal that *Acta1* is differentially upregulated in pathological versus physiological hypertrophy.[130] Exposure to iAS increased *Acta1* mRNA expression in male and not female hearts, in accordance with the hypothesis that iAS induces pathological hypertrophy (Figs. 9a, f). Myosin heavy chain undergoes an isoform shift from its alpha form, *Myh6*, to its beta form, *Myh7*, in the stressed, hypertrophied, and failing hearts.[131–133] Myocardial mRNA levels of *Myh7* and *Myh6* were increased and decreased, respectively, with iAS exposure in male hearts, and no changes were observed in female hearts, further demonstrating that iAS induces pathological hypertrophy (Figs. 9b, c, g, h). Additionally, myocardial mRNA transcripts for ANP, *Nppa*, and BNP, *Nppb*, which are upregulated in cardiac hypertrophy, were increased and unchanged, respectively, in accordance with protein

levels found in plasma (Figs. 5d, e, i, j). Taken together, these data reveal that iAS exposure induces pathological hypertrophy in the male heart.

To determine whether iAS-induced hypertrophy consequently alters myocardial ischemic susceptibility, several hemodynamic parameters were examined using an *ex vivo* model of I/R injury. Cardiac remodeling is an independent risk factor for adverse CV outcomes, and chronic iAS exposure has been particularly well-associated with ischemic heart disease.[98–103,92,72] Furthermore, a previous study from our group highlighted increased I/R injury in remodeled female hearts after a 1000 μg/L iAS exposure for four weeks.[79] As such, it was hypothesized that pathological hypertrophy of heart would increase I/R injury. Male and female hearts were thus subjected to I/R injury via Langendorff perfusion after the eight-week exposure period. However, baseline heart rate, left ventricular developed pressure, contractility, and rate pressure product, as well as post-I/R functional recovery and infarct size did not significantly change with iAS exposure in either sex (Fig. 6). Although iAS-induced pathological hypertrophy did not predispose the male heart to exhibit increased susceptibility to I/R injury, it is possible that this phenotype modulates other CVD risk factors and endpoints, such as QT interval, which have been epidemiologically observed in chronically-exposed populations.[77,134,135] Beyond adverse cardiovascular outcomes in the exposed myocardium, and seeing as several iAS-upregulated transcripts found in this study belong to the fetal gene program, it's interesting to speculate whether a gestational exposure to iAS delays the transition of sarcomeric, metabolic, and contractile proteins into adult isoforms in the postnatal heart to either predispose or induce congenital disease.[136–138]

Considering that iAS-exposed female hearts did not demonstrate cardiovascular pathology throughout this investigation, several sex-dependent targets were probed to determine the

mechanisms that may be responsible for the observed protection. Nitric oxide, produced by endothelial, neuronal, and inducible nitric oxide synthase (eNOS, nNOS, iNOS), serves not only as a signaling molecule in myocardial function, but also as a sex-dependent regulator of myocardial remodeling.[17,39,54,139–143] While eNOS inhibition is shown to induce hypertrophy, abrogated by its restoration, its overexpression is shown to attenuate hypertrophy.[43,44] Furthermore, the antihypertrophic effects of NO manifest in part by cGMP-mediated activation of PKG, which can act through a variety of mechanisms to suppress NFAT transcriptional activity in the myocardium.[21,45,120] Although literature has shown that iAS acts as an endocrine disruptor, some evidence suggests that certain very low doses may upregulate estrogen-mediated gene expression, and as such, it was hypothesized that endogenous female cardioprotection was enhanced by iAS exposure at this timepoint as a quirk of the exposure model.[144] Protein levels of total eNOS and phosphorylated eNOS at S1177, an activating site, did not change with iAS exposure in either sex (Fig. 11). eNOS phosphorylation at T495, an inhibitory site, was decreased in iAS-exposed females, but the increase was not significant when normalized to total eNOS levels (Fig. 11). Additionally, phosphorylation of vasodilator-stimulated phosphoprotein (VASP) at S239, a PKG site, was differentially increased in iAS-exposed females and not in males, but this similarly did not maintain significance when normalized to total VASP levels (Figs. 10). However, the protein levels of PKG and nNOS significantly decreased with iAS exposure in female hearts (Figs. 10, 11). As such, these data suggest that PKG signaling may be impaired as part of the mechanism leading to iAS-induced cardiac remodeling in males, while in females, PKG signaling may be impaired beyond an eight-week exposure.

Further investigation probed upstream mechanisms of how iAS may induce pathological remodeling of the myocardium. Previously, a study reported that a 50 mg/L iAS exposure

for 12 weeks induces systemic hypertension in male rats by increasing the expression of angiotensin II, angiotensin II type I receptor, and angiotensin-converting enzyme.[145] Subsequently, they showed that blocking the receptor ameliorated iAS-induced hypertension and TGF-β-mediated fibrosis.[146] However, considering that current study of an eight-week, 615 μg/L iAS exposure did not find any evidence of myocardial fibrosis, the possibility that iAS directly induces hypertrophy, beyond angiotensin II signaling, was explored. Calcineurin-NFAT signaling is shown to be both necessary and sufficient to induce pathological cardiac hypertrophy.[21,30,120,147] Protein levels of Calcineurin A, the catalytic subunit of the serine-threonine phosphatase, were measured in the myocardium as a crude surrogate for calcineurin-NFAT activation. However, these levels were unchanged with iAS exposure in both sexes (Figs. 12a, b). Regulator of calcineurin 1, *Rcan1*, is an inhibitor of calcineurin A that's upregulated with calcineurin-NFAT activation in a negative feedback loop.[148,149] Measuring its mRNA expression revealed that iAS exposure significantly increased *Rcan1* in the male heart and not in females, in accordance with the phenotype, suggesting that iAS may induce pathological cardiac hypertrophy in part by upregulating the calcineurin-NFAT pathway (Figs. 12c, d).

An *in vitro* model of exposure was established to determine whether iAS activates calcineurin-NFAT signaling independent of blood pressure. Previous studies that have investigated the effects of iAS *in vitro* have determined that the low-level concentrations used for the luciferase assay in the current study increase transcription factor activation and induce gene expression without causing cytotoxicity.[150,151] An MTT cell proliferation assay confirmed the latter (Fig. 12e). Considering that males presented a significantly increased left ventricular anterior wall thickness as well as an increased posterior wall thickness trending towards significance at the fourth week of exposure, prior to any observed increase in

systolic blood pressure, it was hypothesized that iAS can directly induce cardiac hypertrophy. HEK293 cells were transfected with an NFAT-luciferase reporter and plasmids expressing transient receptor potential canonical type 6 (*Trpc6*) and/or Renilla-luciferase as positive and internal controls, respectively.[152,153] Treatment with 1 μM iAS significantly increased NFAT luciferase activity, suggesting that iAS has the potential to induce pathological hypertrophy, independent of blood pressure, through the calcineurin-NFAT pathway (Fig. 12f). Although it appeared that iAS-induced activation of NFAT was biphasic, where 1 μM iAS induced luciferase activity similar to that of the positive control while greater concentrations reduced activity to baseline, previous studies have demonstrated that iAS has an analogous bidirectional, concentration-dependent role in TGF-β/Smad signaling, highlighting nonlinearity underlying the mechanisms of iAS-induced pathology.[104] Taken together, these data suggest that iAS may directly induce pathological cardiac hypertrophy.

iAS has been shown to activate several transcription factors, including nuclear factor erythroid 2-related factor 2 (Nrf2), nuclear factor kappa B (NF-κB), and activating protein-1 (AP-1).[154] Whereas iAS-induced activation of Nrf2 is primarily mediated by the production of reactive oxygen species (ROS), its activation of NF-κB is mediated by both ROS and direct binding of reactive thiols on the inhibitory Keap1 protein.[155] Additionally, iAS has been shown to directly bind zinc finger motifs as well as the AP-1-like transcription factor Yap8, coordinating three critical cysteines to induce an activating conformational change.[155,156] Considering that NFAT is activated by an array of factors, including by proteins with zinc and cysteine-rich domains, by crosstalk with NF-κB, by direct interaction with AP-1, and by ROS, it is beyond the scope of this study to determine the exact iAS-modulated alterations that mediate the hypertrophic response.[157–163] However, it is possible to speculate from literature that iAS-induced activation of NFAT may manifest through combination of

(a) interactions between iAS or an electrophilic iAS metabolite with a reactive thiol of the transcription factor complex, (b) cooperative interactions between NFAT and other transcription factors, and/or (c) oxidative stress.

2.3.1 Limitations

Indeed, this investigation should be considered in the context of its strengths and weaknesses. Although the model of exposure used here doubled the duration of a previous study from our laboratory, the divergence in systolic blood pressure during the last two weeks in iAS-treated males, paired with the lack thereof in females, highlights not only the temporal nature of the CV effects of iAS exposure, but also the limitation of not capturing all such effects in an eight-week study; as such, a longer duration is recommended for future investigations.[79] Additionally, blood pressure was measured using photoplethysmography via tail cuff, which provides indirect readings and serves as another area of potential weakness. However, this tool has been validated for accuracy and reliability by independent study, and it provided sufficient data to extrapolate relative trends, at the least.[164,165] Direct recording of blood pressure via radiotelemetry is a standard that may be used in future studies, given the justification for surgery; this would circumvent the need for restraint and provide continuous measurements with improved accuracy throughout the exposure period.[165] Moreover, while transthoracic echocardiography was conducted at three timepoints throughout this study, additional measurements would provide further resolution. Lastly, the determination of whether iAS-induced hypertrophy altered susceptibility to I/R injury may have utilized an *in vivo* model by surgical occlusion of the left anterior descending coronary artery. Seeing as the present study did not find any alterations in ischemic heart injury, it is recommended that future studies extend this exposure beyond eight weeks such that a hypertrophic phenotype

is observed in both sexes. Additionally, considering the possibility that a chronic, low-level iAS exposure beyond eight weeks induces cardiac hypertrophy and systemic hypertension in both sexes, an optimized exposure model may then investigate the iAS-induced modulation of risk factors to promote CVD pathogenesis.

Notably, this study leverages findings rooted in human populations and begins to unravel a mechanistic understanding using mouse and cell culture systems—an advantage that is also inherently limited by interspecies differences, and as such, the relevance and discrepancy between model systems must be addressed. Animal models provide controlled, organism-level model systems that help evaluate the pathophysiology of environmental exposures by first ideally recapitulating epidemiological phenotypes. Although the iAS dose used in the current study is found among the greater concentrations of exposure in human populations, there exist differences in the methylation and biotransformation of iAS between humans and mice, as well as differences in its rate of excretion, which constructs discrepancies in iAS metabolism and thus the mechanisms of action that may lead to the observed pathologies.[166] Mice demonstrate greater iAS biotransformation and excretion rates compared to humans, but since the difference of the former has been shown to diminish at greater concentrations of iAS in mice compared to humans, it is possible that a mouse exposure to 615 μg/L iAS may induce the effects observed at lower concentrations in humans.[166] Overall, considering that cardiac hypertrophy was observed in the male mouse heart, the mouse exposure model was phenotypically-relevant, in accordance with echocardiography data in humans. Future studies may thus seek to validate these findings in other animal models, such as rats or rabbits, which exhibit even greater rates of iAS biotransformation. Additionally, background co-morbidities such as a high-fat diet, atherosclerosis via apolipoprotein E knockout, or pathological genetic polymorphisms may be utilized to construct a model that recapitulates

relevant risks in human populations, and co-exposures such as other metals or air pollutants may be introduced in order to serve as a more environmentally-relevant model, altogether serving as modes for future investigations examining iAS and the cardiovascular system.

Evaluating the relevance of iAS exposure in a cell culture model is particularly challenging, but the model justifiably served the purpose in the current study to determine whether iAS can activate NFAT independent of an elevation in blood pressure. Cell proliferation was evaluated in order to determine iAS toxicity and ensure that the effects observed were not due to the processes of cell death; this MTT assay (0, 0.5, 1, 5, 10, 25, 50, 100 uM; n = 12 wells/group) revealed that 1 uM iAS treatment for 24 hours did not alter cell proliferation. Additionally, several low-level iAS concentrations were utilized in the luciferase assay, all of which have been evaluated to induce human-relevant expression of oxidative stress genes using the same cell line.[151] Furthermore, iAS-induced gene expression at these concentrations in this cell line has been shown to remain unchanged between six and 24-hour exposures, such that the NFAT activation in the present study is likely not an artifact of time.[151] As such, the novel finding that 1 μM iAS activates NFAT *in vitro* is valid. However, HEK293 cells are derived from human embryonic kidney epithelium, and although these were specifically chosen to yield improved transfection efficiency, they do not share the same proteomic and metabolomic profile compared to cardiomyocytes, and as such, the effect of iAS exposure on the activation of NFAT may be different in the heart. Future studies may thus utilize either a H9C2 rat-derived embryonic cardiac myoblast cell line, which is commercially available, or primary cardiac cells such as neonatal/adult cardiomyocytes or embryonic fibroblasts, isolated from mice, in order to more closely replicate an *in vivo* model of iAS exposure in the myocardium. Additionally, whereas cells were directly treated with iAS in the current study, the fate of iAS ingested through drinking water in targeting

cardiomyocytes may differ in the concentration and/or the metabolite that reaches the heart in mice and humans. Future experiments may thus leverage the novel finding that exposure to iAS induces NFAT activity *in vitro* and further tease out this mechanism by utilizing *in vitro* inhibitors of calcineurin and ROS, among other upstream NFAT activators in order to reduce iAS-induced NFAT transcription back to baseline. Future studies can also provide stronger evidence as to whether iAS exposure *in vivo* directly induces this signaling pathway by utilizing a cardiac-specific NFAT-luciferase reporter mouse. Taken together, since the upregulation of several NFAT targets was observed, in addition to the expected phenotype, there exists justification with the data presented in the current study that iAS exposure may induce cardiac hypertrophy in the mouse heart, at least in part by direct activation of the NFAT pathway.

2.3.4 Conclusions

Overall, this is the first mechanistic investigation examining an environmentally relevant iAS exposure on the development of cardiac hypertrophy in male and female mice. During our eight-week exposure, males showed an increase in systolic blood pressure and altered cardiac geometry, while females appeared to remain protected from such effects. iAS treatment induced an array of molecular changes indicating pathological hypertrophy in the male heart, and these were not detected in female hearts. Further data support the novel finding that iAS induces pathological hypertrophy of the heart in part by activation of the calcineurin-NFAT pathway. Taken together, this investigation provides a mechanistic link between an environmentally relevant iAS exposure, the induction of pathological hypertrophy, and the increased the risk for adverse CV outcomes. Ultimately, these findings underscore the importance of iAS removal from human consumption.

2.3.4 Translational Impact

This study complements clinical findings by highlighting the direct pathophysiological impact of an environmental exposure to iAS on the cardiovascular system. By demonstrating that iAS exposure may cause pathological cardiac hypertrophy by increasing systolic blood pressure, potentially activating calcineurin-NFAT, and inducing the fetal gene program, these results provide novel mechanistic insight into the threat of iAS exposure to the heart, which is necessary to identify targets for medical and public health intervention.

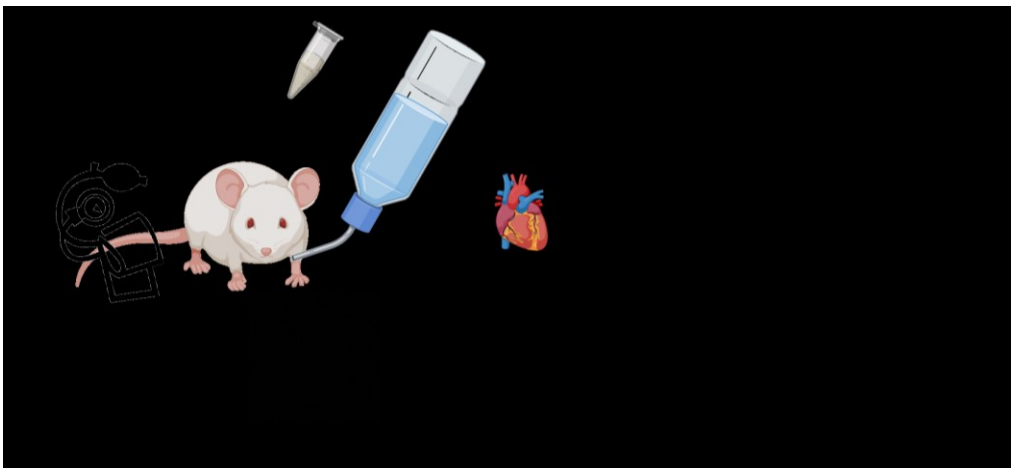

Figure 13. Exposure to iAS induces sex-dependent pathological hypertrophy of the heart. Graphical abstract summarizing the major findings of this investigation.

CHAPTER 3

FUTURE DIRECTIONS

3.1 Optimize the Model of Exposure

Rather than delving into the sex difference characterized in this study and attempting to elucidate a transient mechanism of female cardioprotection, though a notable investigation, future experiments should first and foremost extend the duration of exposure such that cardiac pathology is observed in both males and females as reflected in epidemiological findings. Beyond duration, the present study provides insight into concentrations that should be used in future studies. Results from the luciferase assay suggest that iAS has a biphasic, concentration-dependent effect on NFAT activation. Additionally, the present study utilized observed hypertrophy with no evidence of fibrosis, in direct contrast to previous studies that used several-fold greater concentrations. As such, future studies should contemplate the use of an iAS dose significantly less than 615 μg/L for a longer duration, altogether optimizing an environmentally relevant model of exposure for use in studies investigating the effects of iAS exposure on the cardiovascular system.

3.2 Characterize the Effects on Heart and Cardiomyocyte Physiology

Beyond confirming elevated systolic blood pressure and cardiac remodeling in an optimized exposure model, it'd be particularly interesting to delve into the *in vivo* and *in vitro* physiology of the heart. Characterization of whether iAS exposure decreases myocardial contractility and chamber compliance, which are physiological properties expected in pathological hypertrophy and heart failure that cannot be measured via transthoracic echocardiography, may be achieved by obtaining pressure-volume loops of the anesthetized mouse heart.

Although this was considered for the present study, technical challenges outweighed the insight of the parameters obtained through these detailed hemodynamic measurements. Furthermore, it would be interesting to isolate cardiomyocytes from exposed and control mouse hearts to measure cardiomyocyte contractility and calcium handling. Epidemiological studies have established that iAS exposure is significantly associated with prolongation of the QT interval, which describes a delay between ventricular depolarization and repolarization.[77,167] Mechanistically, this may be the result of an increase in sodium or calcium influx, or a decrease in potassium efflux. Experimental studies have found that iAS exposure increases intracellular calcium levels *in vitro* and alters *in silico* and *in vivo* expression of several calcium binding proteins regulating calcium homeostasis.[168–170] As such, it may be worthwhile to determine whether cardiomyocytes isolated from iAS-exposed hearts exhibit altered calcium transients and shortening. By further characterizing the physiological properties of the iAS-exposed myocardium *in vivo* as well as the *in vitro* cardiac contractile effects of iAS exposure, future investigations may provide a deeper understanding of the mechanisms by which iAS exposure alters cardiovascular physiology to increase CVD susceptibility and pathogenesis.

3.3 Define the Effects of Inorganic Arsenic on NFAT Activation

Considering that the present study highlights the potential for calcineurin-NFAT activation in the induction of pathological hypertrophy, it is also logical to next define the mechanisms through which activation may manifest. Preliminary experimentation should characterize the phosphorylation and localization of NFAT and its isoforms as permitted by the antibodies available; a decrease in phosphorylation and an increase in nuclear localization is expected with increased calcineurin activity in pathological cardiac hypertrophy. Additionally, it would

be worthwhile to probe the levels of negative calcineurin-NFAT regulators such as glycogen synthase kinase 3 beta, which phosphorylates NFAT to enhance its nuclear export and cytosolic localization. Upstream factors that may activate this signaling pathway center around increased intracellular calcium such that iAS-exposed hearts may exhibit increased modification of calmodulin target proteins. Furthermore, an *in vitro* approach to determine whether iAS activates NFAT by increasing intracellular calcium may be to observe whether iAS-treated H9C2 cardiac cells display NFAT luciferase activity with a calcium channel blocker. Separately, seeing as iAS may activate NFAT by promoting cooperativity with other iAS-activated transcription factors, by directly interacting with the transcription factor complex, or by inducing ROS, several additional *in vitro* approaches may be taken. Whether iAS induces cooperativity with other transcription factors such as NF-κB or AP-1 to activate NFAT may be determined by an electrophoretic mobility shift assay or a fluorescence resonance energy transfer experiment. Whether iAS directly interacts with NFAT to upregulate its targets may be determined by treating H9C2 cells with biotinylated iAS and running a pull-down with streptavidin to then identify via liquid chromatography MS/MS whether any NFAT isoforms are bound. Lastly, to determine whether ROS-mediated activation of NFAT is responsible for iAS-induced hypertrophy, NFAT luciferase activity in iAS-treated H9C2 cells may be observed in the presence of ROS scavengers. Indeed, an investigation to determine the mechanism by which iAS activates NFAT is complex, but any combination of these proposed experiments will provide critical insight into the effect of iAS exposure in modulating the cardiovascular system in health and disease.

3.5 Explore the Effects of Inorganic Arsenic on the Developing Heart

Several iAS-upregulated transcripts found in the present study belong to the fetal gene program, and as such, it is interesting to speculate whether a gestational exposure to iAS delays the transition of sarcomeric, metabolic, and contractile proteins into adult isoforms in the postnatal heart to either predispose or induce congenital disease.[136–138] Metabolism in the fetal heart leverages carbohydrates such as glucose, lactate, and glycogen as the primary substrate for energy, rather than fatty acids as used by the adult heart. Additionally, contractile physiology of the fetal heart is geared towards mechanical performance under fetal circulation and thus, for example, utilizes slow twitch muscle fibers rather than the fast twitch isoform found in the adult heart. Exposure to iAS is herein observed to induce a panel of myocardial mRNA transcripts that suggests a return to the fetal gene program. As such, a future study should determine whether a maternal exposure to iAS throughout pregnancy activates and prolongs the expression of these genes in both the fetal and postnatal heart. Perhaps the measurement of fetal gene expression across the developmental stages of the iAS-exposed heart through birth may indicate a delay the switch to expressing isoforms required in the adult heart, thereby priming the progeny for structural and metabolic abnormalities associated with an increased CVD susceptibility. Again, these experiments are technically challenging, but taken together, may provide novel understanding of how iAS may modulate a lifetime of increased risk to pathologies of the cardiovascular system.

REFERENCES

1. Archer, E. & Blair, S. N. Physical Activity and the Prevention of Cardiovascular Disease: From Evolution to Epidemiology. *Progress in Cardiovascular Diseases* **53**, 387–396 (2011).
2. Finegold, J. A., Asaria, P. & Francis, D. P. Mortality from ischaemic heart disease by country, region, and age: Statistics from World Health Organisation and United Nations. *International Journal of Cardiology* **168**, 934–945 (2013).
3. Piepoli, M. F. *et al.* 2016 European Guidelines on cardiovascular disease prevention in clinical practice: The Sixth Joint Task Force of the European Society of Cardiology and Other Societies on Cardiovascular Disease Prevention in Clinical Practice (constituted by representatives of 10 societies and by invited experts)Developed with the special contribution of the European Association for Cardiovascular Prevention & Rehabilitation (EACPR). *European Heart Journal* **37**, 2315–2381 (2016).
4. Mosca Lori, Barrett-Connor Elizabeth & Kass Wenger Nanette. Sex/Gender Differences in Cardiovascular Disease Prevention. *Circulation* **124**, 2145–2154 (2011).
5. Cosselman, K. E., Navas-Acien, A. & Kaufman, J. D. Environmental factors in cardiovascular disease. *Nature Reviews Cardiology* **12**, 627–642 (2015).
6. Roth, G. A. *et al.* Global, regional, and national age-sex-specific mortality for 282 causes of death in 195 countries and territories, 1980–2017: a systematic analysis for the Global Burden of Disease Study 2017. *The Lancet* **392**, 1736–1788 (2018).
7. Murray, C. J. L. & Lopez, A. D. Measuring the Global Burden of Disease. *New England Journal of Medicine* **369**, 448–457 (2013).
8. Virani Salim S. *et al.* Heart Disease and Stroke Statistics—2020 Update. *Circulation* **0**, CIR.0000000000000757.

9. Luczak, E. D. & Leinwand, L. A. Sex-based cardiac physiology. *Annu. Rev. Physiol.* **71**, 1–18 (2009).

10. Vrtačnik, P., Ostanek, B., Mencej-Bedrač, S. & Marc, J. The many faces of estrogen signaling. *Biochem Med (Zagreb)* **24**, 329–342 (2014).

11. Higginbotham M B, Morris K G, Coleman R E & Cobb F R. Sex-related differences in the normal cardiac response to upright exercise. *Circulation* **70**, 357–366 (1984).

12. Sullivan, M. J., Cobb, F. R. & Higginbotham, M. B. Stroke volume increases by similar mechanisms during upright exercise in normal men and women. *American Journal of Cardiology* **67**, 1405–1412 (1991).

13. Huxley, V. H. Sex and the cardiovascular system: the intriguing tale of how women and men regulate cardiovascular function differently. *Adv Physiol Educ* **31**, 17–22 (2007).

14. Sanghavi Monika & Rutherford John D. Cardiovascular Physiology of Pregnancy. *Circulation* **130**, 1003–1008 (2014).

15. Shufelt, C., Pacheco, C., Tweet, M. S. & Miller, V. M. Sex-specific physiology and cardiovascular disease. *Adv Exp Med Biol* **1065**, 433–454 (2018).

16. Lam, C. S. P. *et al.* Sex differences in heart failure. *Eur. Heart J.* **40**, 3859–3868c (2019).

17. Casin, K. M. & Kohr, M. J. An emerging perspective on sex differences: Intersecting S-nitrosothiol and aldehyde signaling in the heart. *Redox Biology* 101441 (2020) doi:10.1016/j.redox.2020.101441.

18. Shioi, T. *et al.* Akt/protein kinase B promotes organ growth in transgenic mice. *Mol. Cell. Biol.* **22**, 2799–2809 (2002).

19. McMullen, J. R. *et al.* Phosphoinositide 3-kinase(p110alpha) plays a critical role for the induction of physiological, but not pathological, cardiac hypertrophy. *Proc. Natl. Acad. Sci. U.S.A.* **100**, 12355–12360 (2003).

20. McMullen, J. R. *et al.* The insulin-like growth factor 1 receptor induces physiological heart growth via the phosphoinositide 3-kinase(p110alpha) pathway. *J. Biol. Chem.* **279**, 4782–4793 (2004).

21. Nakamura, M. & Sadoshima, J. Mechanisms of physiological and pathological cardiac hypertrophy. *Nature Reviews Cardiology* **15**, 387–407 (2018).

22. Levy, D., Garrison, R. J., Savage, D. D., Kannel, W. B. & Castelli, W. P. Prognostic implications of echocardiographically determined left ventricular mass in the Framingham Heart Study. *N. Engl. J. Med.* **322**, 1561–1566 (1990).

23. Koren, M. J., Devereux, R. B., Casale, P. N., Savage, D. D. & Laragh, J. H. Relation of left ventricular mass and geometry to morbidity and mortality in uncomplicated essential hypertension. *Ann. Intern. Med.* **114**, 345–352 (1991).

24. Brown, D. W., Giles, W. H. & Croft, J. B. Left ventricular hypertrophy as a predictor of coronary heart disease mortality and the effect of hypertension. *Am. Heart J.* **140**, 848–856 (2000).

25. Ferdinandy, P., Schulz, R. & Baxter, G. F. Interaction of Cardiovascular Risk Factors with Myocardial Ischemia/Reperfusion Injury, Preconditioning, and Postconditioning. *Pharmacological Reviews* **59**, 418–458 (2007).

26. Friehs, I. & del Nido, P. J. Increased susceptibility of hypertrophied hearts to ischemic injury. *The Annals of Thoracic Surgery* **75**, S678–S684 (2003).

27. Frey, N. & Olson, E. N. Cardiac Hypertrophy: The Good, the Bad, and the Ugly. *Annual Review of Physiology* **65**, 45–79 (2003).

28. Olson, E. N. & Williams, R. S. Calcineurin Signaling and Muscle Remodeling. *Cell* **101**, 689–692 (2000).

29. Crabtree, G. R. & Olson, E. N. NFAT Signaling: Choreographing the Social Lives of Cells. *Cell* **109**, S67–S79 (2002).

30. Molkentin, J. D. *et al.* A Calcineurin-Dependent Transcriptional Pathway for Cardiac Hypertrophy. *Cell* **93**, 215–228 (1998).

31. Heineke, J. & Molkentin, J. D. Regulation of cardiac hypertrophy by intracellular signalling pathways. *Nature Reviews Molecular Cell Biology* **7**, 589–600 (2006).

32. Pinto Alexander R. *et al.* Revisiting Cardiac Cellular Composition. *Circulation Research* **118**, 400–409 (2016).

33. Ma, Z.-G., Yuan, Y.-P., Wu, H.-M., Zhang, X. & Tang, Q.-Z. Cardiac fibrosis: new insights into the pathogenesis. *Int J Biol Sci* **14**, 1645–1657 (2018).

34. Weber, K. T. Cardiac interstitium in health and disease: the fibrillar collagen network. *J. Am. Coll. Cardiol.* **13**, 1637–1652 (1989).

35. Cleutjens, J. P., Verluyten, M. J., Smiths, J. F. & Daemen, M. J. Collagen remodeling after myocardial infarction in the rat heart. *Am J Pathol* **147**, 325–338 (1995).

36. Kong, P., Christia, P. & Frangogiannis, N. G. The Pathogenesis of Cardiac Fibrosis. *Cell Mol Life Sci* **71**, 549–574 (2014).

37. López Begoña, Querejeta Ramón, González Arantxa, Larman Mariano & Díez Javier. Collagen Cross-Linking But Not Collagen Amount Associates With Elevated Filling Pressures in Hypertensive Patients With Stage C Heart Failure. *Hypertension* **60**, 677–683 (2012).

38. Woodiwiss A. J. *et al.* Reduction in Myocardial Collagen Cross-Linking Parallels Left Ventricular Dilatation in Rat Models of Systolic Chamber Dysfunction. *Circulation* **103**, 155–160 (2001).

39. Ziolo, M. T., Kohr, M. J. & Wang, H. Nitric oxide signaling and the regulation of myocardial function. *Journal of Molecular and Cellular Cardiology* **45**, 625–632 (2008).

40. Calvert, J. W. *et al.* Exercise protects against myocardial ischemia-reperfusion injury via stimulation of β(3)-adrenergic receptors and increased nitric oxide signaling: role of nitrite and nitrosothiols. *Circ. Res.* **108**, 1448–1458 (2011).

41. Shesely, E. G. *et al.* Elevated blood pressures in mice lacking endothelial nitric oxide synthase. *Proc. Natl. Acad. Sci. U.S.A.* **93**, 13176–13181 (1996).

42. Lee, P. C. *et al.* Impaired wound healing and angiogenesis in eNOS-deficient mice. *American Journal of Physiology-Heart and Circulatory Physiology* **277**, H1600–H1608 (1999).

43. Umar, S. & van der Laarse, A. Nitric oxide and nitric oxide synthase isoforms in the normal, hypertrophic, and failing heart. *Molecular and Cellular Biochemistry* **333**, 191–201 (2010).

44. Massion, P. B. & Balligand, J.-L. Relevance of nitric oxide for myocardial remodeling. *Current Heart Failure Reports* **4**, 18–25 (2007).

45. Fiedler, B. *et al.* Inhibition of calcineurin-NFAT hypertrophy signaling by cGMP-dependent protein kinase type I in cardiac myocytes. *Proceedings of the National Academy of Sciences* **99**, 11363–11368 (2002).

46. Lukowski, R. *et al.* Cardiac hypertrophy is not amplified by deletion of cGMP-dependent protein kinase I in cardiomyocytes. *Proceedings of the National Academy of Sciences* **107**, 5646–5651 (2010).

47. Braunwald, E. & Kloner, R. A. Myocardial reperfusion: a double-edged sword? *Journal of Clinical Investigation* **76**, 1713–1719 (1985).

48. Kerrigan, C. L. & Stotland, M. A. Ischemia reperfusion injury: A review. *Microsurgery* **14**, 165–175 (1993).

49. Buja, L. M. Myocardial ischemia and reperfusion injury. *Cardiovascular Pathology* **14**, 170–175 (2005).

50. Yellon, D. M. & Hausenloy, D. J. Myocardial Reperfusion Injury. *The New England Journal of Medicine* 15 (2007).

51. Hausenloy, D. J. & Yellon, D. M. Myocardial ischemia-reperfusion injury: a neglected therapeutic target. *Journal of Clinical Investigation* **123**, 92–100 (2013).

52. Bolli, R. *et al.* Myocardial Protection at a Crossroads: The Need for Translation Into Clinical Therapy. *Circulation Research* **95**, 125–134 (2004).

53. Chambliss, K. L. & Shaul, P. W. Estrogen Modulation of Endothelial Nitric Oxide Synthase. *Endocrine Reviews* **23**, 665–686 (2002).

54. Jones, S. P. & Bolli, R. The ubiquitous role of nitric oxide in cardioprotection. *Journal of Molecular and Cellular Cardiology* **40**, 16–23 (2006).

55. Vahter, M., Åkesson, A., Lidén, C., Ceccatelli, S. & Berglund, M. Gender differences in the disposition and toxicity of metals. *Environmental Research* **104**, 85–95 (2007).

56. Murphy, E., Kohr, M., Sun, J., Nguyen, T. & Steenbergen, C. S-nitrosylation: A radical way to protect the heart. *Journal of Molecular and Cellular Cardiology* **52**, 568–577 (2012).

57. Casin Kevin M. *et al.* S-Nitrosoglutathione Reductase Is Essential for Protecting the Female Heart From Ischemia-Reperfusion Injury. *Circulation Research* **123**, 1232–1243 (2018).

58. Lin, J., Steenbergen, C., Murphy, E. & Sun, J. Estrogen receptor beta (ER-β) activation results in S-nitrosylation of proteins involved in cardioprotection. *Circulation* **120**, 245–254 (2009).

59. Sun Junhui *et al.* Hypercontractile Female Hearts Exhibit Increased S-Nitrosylation of the L-Type Ca2+ Channel α1 Subunit and Reduced Ischemia/Reperfusion Injury. *Circulation Research* **98**, 403–411 (2006).

60. Inserte, J. & Garcia-Dorado, D. The cGMP/PKG pathway as a common mediator of cardioprotection: translatability and mechanism: cGMP/PKG-mediated cardioprotection. *British Journal of Pharmacology* **172**, 1996–2009 (2015).

61. González, D. R. *et al.* Differential role of S-nitrosylation and the NO–cGMP–PKG pathway in cardiac contractility. *Nitric Oxide* **18**, 157–167 (2008).

62. Murphy, E. & Steenbergen, C. Mechanisms Underlying Acute Protection From Cardiac Ischemia-Reperfusion Injury. *Physiological Reviews* **88**, 581–609 (2008).

63. Heusch, G., Boengler, K. & Schulz, R. Cardioprotection: Nitric Oxide, Protein Kinases, and Mitochondria. *Circulation* **118**, 1915–1919 (2008).

64. Miller, M. R. & Newby, D. E. Air pollution and cardiovascular disease: car sick. *Cardiovasc Res* **116**, 279–294 (2020).

65. Münzel, T. Up in the air: links between the environment and cardiovascular disease. *Cardiovasc Res* **115**, e144–e146 (2019).

66. Lelieveld, J. *et al.* Loss of life expectancy from air pollution compared to other risk factors: a worldwide perspective. *Cardiovasc Res* doi:10.1093/cvr/cvaa025.

67. Bhatnagar Aruni. Environmental Determinants of Cardiovascular Disease. *Circulation Research* **121**, 162–180 (2017).

68. Smedley, P. L. & Kinniburgh, D. G. A review of the source, behaviour and distribution of arsenic in natural waters. *Applied Geochemistry* **17**, 517–568 (2002).

69. Navas-Acien, A. & Nachman, K. E. Public Health Responses to Arsenic in Rice and Other Foods. *JAMA Intern Med* **173**, 1395–1396 (2013).

70. Naujokas, M. F. *et al.* The Broad Scope of Health Effects from Chronic Arsenic Exposure: Update on a Worldwide Public Health Problem. *Environmental Health Perspectives* **121**, 295–302 (2013).

71. Hughes, M. F., Beck, B. D., Chen, Y., Lewis, A. S. & Thomas, D. J. Arsenic Exposure and Toxicology: A Historical Perspective. *Toxicol Sci* **123**, 305–332 (2011).

72. Moon, K. A. *et al.* A dose-response meta-analysis of chronic arsenic exposure and incident cardiovascular disease. *Int J Epidemiol* **46**, 1924–1939 (2017).

73. Carmignani, M., Boscolo, P. & Castellino, N. Metabolic Fate and Cardiovascular Effects of Arsenic in Rats and Rabbits Chronically Exposed to Trivalent and Pentavalent Arsenic. in *Receptors and Other Targets for Toxic Substances* (eds. Chambers, P. L., Cholnoky, E. & Chambers, C. M.) 452–455 (Springer Berlin Heidelberg, 1985).

74. Sanchez-Soria, P., Broka, D., Monks, S. L. & Camenisch, T. D. Chronic Low-Level Arsenite Exposure through Drinking Water Increases Blood Pressure and Promotes Concentric Left Ventricular Hypertrophy in Female Mice. *Toxicologic Pathology* **40**, 504–512 (2012).

75. Kwok, R. K. *et al.* Drinking water arsenic exposure and blood pressure in healthy women of reproductive age in Inner Mongolia, China. *Toxicology and Applied Pharmacology* **222**, 337–343 (2007).

76. Osorio-Yáñez, C. *et al.* Blood Pressure, Left Ventricular Geometry, and Systolic Function in Children Exposed to Inorganic Arsenic. *Environmental Health Perspectives* **123**, 629–635 (2015).

77. Chen, Y. *et al.* Arsenic Exposure from Drinking Water and QT-Interval Prolongation: Results from the Health Effects of Arsenic Longitudinal Study. *Environmental Health Perspectives* **121**, 427–432 (2013).

78. Kumagai, Y. & Pi, J. Molecular basis for arsenic-Induced alteration in nitric oxide production and oxidative stress: implication of endothelial dysfunction. *Toxicology and Applied Pharmacology* **198**, 450–457 (2004).

79. Veenema, R. J. *et al.* Inorganic Arsenic Exposure Induces Sex Disparate Effects and Exacerbates Ischemia-Reperfusion Injury in the Female Heart. *American Journal of Physiology-Heart and Circulatory Physiology* (2019) doi:10.1152/ajpheart.00364.2018.

80. Murphy, E. & Steenbergen, C. Gender-based differences in mechanisms of protection in myocardial ischemia–reperfusion injury. *Cardiovasc Res* **75**, 478–486 (2007).

81. Wang, M. *et al.* Role of endogenous testosterone in myocardial proinflammatory and proapoptotic signaling after acute ischemia-reperfusion. *American Journal of Physiology-Heart and Circulatory Physiology* **288**, H221–H226 (2005).

82. Wang, M., Baker, L., Tsai, B. M., Meldrum, K. K. & Meldrum, D. R. Sex differences in the myocardial inflammatory response to ischemia-reperfusion injury. *American Journal of Physiology-Endocrinology and Metabolism* **288**, E321–E326 (2005).

83. Brown, D. A. *et al.* Susceptibility of the heart to ischaemia–reperfusion injury and exercise-induced cardioprotection are sex-dependent in the rat. *The Journal of Physiology* **564**, 619–630 (2005).

84. Bae, S. & Zhang, L. Gender Differences in Cardioprotection against Ischemia/Reperfusion Injury in Adult Rat Hearts: Focus on Akt and Protein Kinase C Signaling. *J Pharmacol Exp Ther* **315**, 1125–1135 (2005).

85. Chen Chien-Jen, Chiou Hung-Yi, Chiang Ming-Hsi, Lin Li-Ju & Tai Tong-Yuan. Dose-Response Relationship Between Ischemic Heart Disease Mortality and Long-term Arsenic Exposure. *Arteriosclerosis, Thrombosis, and Vascular Biology* **16**, 504–510 (1996).

86. Moran Andrew E. *et al.* Temporal Trends in Ischemic Heart Disease Mortality in 21 World Regions, 1980 to 2010. *Circulation* **129**, 1483–1492 (2014).

87. Benjamin Emelia J. *et al.* Heart Disease and Stroke Statistics—2018 Update: A Report From the American Heart Association. *Circulation* **137**, e67–e492 (2018).

88. Arnett, D. K. *et al.* 2019 ACC/AHA Guideline on the Primary Prevention of Cardiovascular Disease: A Report of the American College of Cardiology/American Heart Association Task Force on Clinical Practice Guidelines. *J Am Coll Cardiol* **74**, e177–e232 (2019).

89. Kapaj, S., Peterson, H., Liber, K. & Bhattacharya, P. Human health effects from chronic arsenic poisoning--a review. *J Environ Sci Health A Tox Hazard Subst Environ Eng* **41**, 2399–2428 (2006).

90. Mohammed Abdul, K. S., Jayasinghe, S. S., Chandana, E. P. S., Jayasumana, C. & De Silva, P. M. C. S. Arsenic and human health effects: A review. *Environmental Toxicology and Pharmacology* **40**, 828–846 (2015).

91. Moon, K., Guallar, E. & Navas-Acien, A. Arsenic Exposure and Cardiovascular Disease:An Updated Systematic Review. *Current Atherosclerosis Reports* **14**, 542–555 (2012).

92. Moon, K. A. *et al.* Association Between Exposure to Low to Moderate Arsenic Levels and Incident Cardiovascular Disease: A Prospective Cohort Study. *Ann Intern Med* (2013) doi:10.7326/0003-4819-159-10-201311190-00719.

93. Pichler Gernot *et al.* Association of Arsenic Exposure With Cardiac Geometry and Left Ventricular Function in Young Adults. *Circulation: Cardiovascular Imaging* **12**, e009018 (2019).

94. Nestle Pure Life 2017 Water Analysis Report.

95. Murko, M., Elek, B., Styblo, M., Thomas, D. J. & Francesconi, K. A. Dose and Diet – Sources of Arsenic Intake in Mouse *in Utero* Exposure Scenarios. *Chemical Research in Toxicology* **31**, 156–164 (2018).

96. Bell, R. M., Mocanu, M. M. & Yellon, D. M. Retrograde heart perfusion: The Langendorff technique of isolated heart perfusion. *Journal of Molecular and Cellular Cardiology* **50**, 940–950 (2011).

97. Mitchell, J. R. *et al.* Short-term dietary restriction and fasting precondition against ischemia reperfusion injury in mice. *Aging Cell* **9**, 40–53 (2010).

98. Kannel, W. B. Left ventricular hypertrophy as a risk factor: the Framingham experience. *J Hypertens Suppl* **9**, S3-8; discussion S8-9 (1991).

99. Gjesdal, O., Bluemke, D. A. & Lima, J. A. Cardiac remodeling at the population level—risk factors, screening, and outcomes. *Nature Reviews Cardiology* **8**, 673–685 (2011).

100. Azevedo, P. S., Polegato, B. F., Minicucci, M. F., Paiva, S. A. R. & Zornoff, L. A. M. Cardiac Remodeling: Concepts, Clinical Impact, Pathophysiological Mechanisms and Pharmacologic Treatment. *Arq Bras Cardiol* **106**, 62–69 (2016).

101. Gerdts, E. *et al.* Left ventricular hypertrophy offsets the sex difference in cardiovascular risk (the Campania Salute Network). *International Journal of Cardiology* **258**, 257–261 (2018).

102. Tseng, C.-H. *et al.* Long-term arsenic exposure and ischemic heart disease in arseniasis-hyperendemic villages in Taiwan. *Toxicology Letters* **137**, 15–21 (2003).

103. Chen, Y. *et al.* Arsenic exposure from drinking water and mortality from cardiovascular disease in Bangladesh: prospective cohort study. *BMJ* **342**, (2011).

104. Dai, J. *et al.* Bi-directional regulation of TGF-β/Smad pathway by arsenic: A systemic review and meta-analysis of in vivo and in vitro studies. *Life Sciences* **220**, 92–105 (2019).

105. Jiang Jieying *et al.* Association between Arsenic Exposure from Drinking Water and Longitudinal Change in Blood Pressure among HEALS Cohort Participants. *Environmental Health Perspectives* **123**, 806–812 (2015).

106. Mordukhovich Irina *et al.* Associations of Toenail Arsenic, Cadmium, Mercury, Manganese, and Lead with Blood Pressure in the Normative Aging Study. *Environmental Health Perspectives* **120**, 98–104 (2012).

107. Rahman Mahfuzar *et al.* Hypertension and Arsenic Exposure in Bangladesh. *Hypertension* **33**, 74–78 (1999).

108. Kunrath, J. *et al.* Blood pressure hyperreactivity: an early cardiovascular risk in normotensive men exposed to low-to-moderate inorganic arsenic in drinking water. *J Hypertens* **31**, 361–369 (2013).

109. Zhang, C. *et al.* Relationship between long-term exposure to low-level arsenic in drinking water and the prevalence of abnormal blood pressure. *Journal of Hazardous Materials* **262**, 1154–1158 (2013).

110. Yang, H.-T., Chou, H.-J., Han, B.-C. & Huang, S.-Y. Lifelong inorganic arsenic compounds consumption affected blood pressure in rats. *Food and Chemical Toxicology* **45**, 2479–2487 (2007).

111. Yin, F. C., Spurgeon, H. A., Rakusan, K., Weisfeldt, M. L. & Lakatta, E. G. Use of tibial length to quantify cardiac hypertrophy: application in the aging rat. *American Journal of Physiology-Heart and Circulatory Physiology* **243**, H941–H947 (1982).

112. Song, W., Wang, H. & Wu, Q. Atrial Natriuretic Peptide in Cardiovascular Biology and Disease (NPPA). *Gene* **569**, 1–6 (2015).

113. Kerkelä, R., Ulvila, J. & Magga, J. Natriuretic Peptides in the Regulation of Cardiovascular Physiology and Metabolic Events. *J Am Heart Assoc* **4**, (2015).

114. John, S. W. *et al.* Genetic decreases in atrial natriuretic peptide and salt-sensitive hypertension. *Science* **267**, 679–681 (1995).

115. Holtwick, R. *et al.* Pressure-independent cardiac hypertrophy in mice with cardiomyocyte-restricted inactivation of the atrial natriuretic peptide receptor guanylyl cyclase-A. *J Clin Invest* **111**, 1399–1407 (2003).

116. Tamura, N. *et al.* Cardiac fibrosis in mice lacking brain natriuretic peptide. *Proc Natl Acad Sci U S A* **97**, 4239–4244 (2000).

117. Kapoun Ann M. *et al.* B-Type Natriuretic Peptide Exerts Broad Functional Opposition to Transforming Growth Factor-β in Primary Human Cardiac Fibroblasts. *Circulation Research* **94**, 453–461 (2004).

118. Khalil, H. *et al.* Fibroblast-specific TGF-β–Smad2/3 signaling underlies cardiac fibrosis. *J Clin Invest* **127**, 3770–3783.

119. Bhandary Bidur *et al.* Cardiac Fibrosis in Proteotoxic Cardiac Disease is Dependent Upon Myofibroblast TGF-β Signaling. *Journal of the American Heart Association* **7**, e010013 (2018).

120. Shimizu, I. & Minamino, T. Physiological and pathological cardiac hypertrophy. *Journal of Molecular and Cellular Cardiology* **97**, 245–262 (2016).

121. Liu, L.-Z. *et al.* Role and Mechanism of Arsenic in Regulating Angiogenesis. *PLOS ONE* **6**, e20858 (2011).

122. Carpenter, R. L. *et al.* Arsenite induces cell transformation by reactive oxygen species, AKT, ERK1/2, and p70S6K1. *Biochemical and Biophysical Research Communications* **414**, 533–538 (2011).

123. Liu, J., Chen, B., Lu, Y., Guan, Y. & Chen, F. JNK-Dependent Stat3 Phosphorylation Contributes to Akt Activation in Response to Arsenic Exposure. *Toxicol Sci* **129**, 363–371 (2012).

124. Beezhold, K. *et al.* miR-190-Mediated Downregulation of PHLPP Contributes to Arsenic-Induced Akt Activation and Carcinogenesis. *Toxicol Sci* **123**, 411–420 (2011).

125. Gao, N. *et al.* Arsenite induces HIF-1α and VEGF through PI3K, Akt and reactive oxygen species in DU145 human prostate carcinoma cells. *Mol Cell Biochem* **255**, 33–45 (2004).

126. Ouyang Weiming *et al.* PI-3K/Akt Pathway-Dependent Cyclin D1 Expression Is Responsible for Arsenite-Induced Human Keratinocyte Transformation. *Environmental Health Perspectives* **116**, 1–6 (2008).

127. Schwartz K *et al.* Alpha-skeletal muscle actin mRNA's accumulate in hypertrophied adult rat hearts. *Circulation Research* **59**, 551–555 (1986).

128. Suurmeijer, A. J. *et al.* α-Actin isoform distribution in normal and failing human heart: a morphological, morphometric, and biochemical study. *The Journal of Pathology* **199**, 387–397 (2003).

129. Driesen, R. B. *et al.* Re-expression of alpha skeletal actin as a marker for dedifferentiation in cardiac pathologies. *J Cell Mol Med* **13**, 896–908 (2009).

130. Song, H. K., Hong, S.-E., Kim, T. & Kim, D. H. Deep RNA Sequencing Reveals Novel Cardiac Transcriptomic Signatures for Physiological and Pathological Hypertrophy. *PLOS ONE* **7**, e35552 (2012).

131. Nakao, K., Minobe, W., Roden, R., Bristow, M. R. & Leinwand, L. A. Myosin heavy chain gene expression in human heart failure. *J Clin Invest* **100**, 2362–2370 (1997).

132. Krenz, M. & Robbins, J. Impact of beta-myosin heavy chain expression on cardiac function during stress. *Journal of the American College of Cardiology* **44**, 2390–2397 (2004).

133. Gupta, M. P. Factors controlling cardiac myosin-isoform shift during hypertrophy and heart failure. *J Mol Cell Cardiol* **43**, 388–403 (2007).

134. Kang, Y. J. Cardiac Hypertrophy: A Risk Factor for QT-Prolongation and Cardiac Sudden Death. *Toxicol Pathol* **34**, 58–66 (2006).

135. Mumford, J. L. *et al.* Chronic Arsenic Exposure and Cardiac Repolarization Abnormalities with QT Interval Prolongation in a Population-based Study. *Environ Health Perspect* **115**, 690–694 (2007).

136. Rudnai, T. *et al.* Arsenic in drinking water and congenital heart anomalies in Hungary. *International Journal of Hygiene and Environmental Health* **217**, 813–818 (2014).

137. Jin, X. *et al.* Maternal exposure to arsenic and cadmium and the risk of congenital heart defects in offspring. *Reproductive Toxicology* **59**, 109–116 (2016).

138. Lin, Y. *et al.* Embryonic protective role of folate in arsenic-induced cardiac malformations in rats. *Int J Clin Exp Pathol* **11**, 1946–1955 (2018).

139. Wollert, K. C. & Drexler, H. Regulation of Cardiac Remodeling by Nitric Oxide: Focus on Cardiac Myocyte Hypertrophy and Apoptosis. *Heart Fail Rev* **7**, 317–325 (2002).

140. Ruiz-Hurtado, G. & Delgado, C. Nitric oxide pathway in hypertrophied heart: new therapeutic uses of nitric oxide donors. *Journal of Hypertension* **28**, S56 (2010).

141. Wong, P. G., Armstrong, D. W. J., Tse, M. Y., Ventura, N. M. & Pang, S. C. Contribution of Estrogen to Sex Dimorphic Expression of Cardiac Natriuretic Peptide and Nitric Oxide Synthase Systems in ANP Gene-Disrupted Mice. *Open Journal of Endocrine and Metabolic Diseases* **3**, 1–11 (2013).

142. Davidson, S. M. & Yellon, D. M. Cardioprotection – is no the answer? A renewed look at nitric oxide signalling in cardiomyocytes. *Cardiovasc Res* **114**, 773–775 (2018).

143. Tong Dan *et al.* Female Sex Is Protective in a Preclinical Model of Heart Failure With Preserved Ejection Fraction. *Circulation* **140**, 1769–1771 (2019).

144. Davey, J. C., Bodwell, J. E., Gosse, J. A. & Hamilton, J. W. Arsenic as an Endocrine Disruptor: Effects of Arsenic on Estrogen Receptor–Mediated Gene Expression In Vivo and in Cell Culture. *Toxicol Sci* **98**, 75–86 (2007).

145. Waghe, P. *et al.* Arsenic causes aortic dysfunction and systemic hypertension in rats: Augmentation of angiotensin II signaling. *Chemico-Biological Interactions* **237**, 104–114 (2015).

146. Khuman, M. W. *et al.* Candesartan ameliorates arsenic-induced hypertensive vascular remodeling by regularizing angiotensin II and TGF-beta signaling in rats. *Toxicology* **374**, 29–41 (2016).

147. Wilkins Benjamin J. *et al.* Calcineurin/NFAT Coupling Participates in Pathological, but not Physiological, Cardiac Hypertrophy. *Circulation Research* **94**, 110–118 (2004).

148. Vega, R. B., Yang, J., Rothermel, B. A., Bassel-Duby, R. & Williams, R. S. Multiple Domains of MCIP1 Contribute to Inhibition of Calcineurin Activity. *J. Biol. Chem.* **277**, 30401–30407 (2002).

149. Chan, B., Greenan, G., McKeon, F. & Ellenberger, T. Identification of a peptide fragment of DSCR1 that competitively inhibits calcineurin activity in vitro and in vivo. *PNAS* **102**, 13075–13080 (2005).

150. Barchowsky, A., Klei, L. R., Dudek, E. J., Swartz, H. M. & James, P. E. Stimulation of reactive oxygen, but not reactive nitrogen species, in vascular endothelial cells exposed to low levels of arsenite. *Free Radical Biology and Medicine* **27**, 1405–1412 (1999).

151. Zheng, X. H., Watts, G. S., Vaught, S. & Gandolfi, A. J. Low-level arsenite induced gene expression in HEK293 cells. *Toxicology* **187**, 39–48 (2003).

152. Makarewich Catherine A. *et al.* Transient Receptor Potential Channels Contribute to Pathological Structural and Functional Remodeling After Myocardial Infarction. *Circulation Research* **115**, 567–580 (2014).

153. Koitabashi, N. *et al.* Cyclic GMP/PKG-dependent inhibition of TRPC6 channel activity and expression negatively regulates cardiomyocyte NFAT activation: Novel mechanism of cardiac stress modulation by PDE5 inhibition. *Journal of Molecular and Cellular Cardiology* **48**, 713–724 (2010).

154. Kumagai, Y. & Sumi, D. Arsenic: Signal Transduction, Transcription Factor, and Biotransformation Involved in Cellular Response and Toxicity. *Annual Review of Pharmacology and Toxicology* **47**, 243–262 (2007).

155. Kumar, N. V. *et al.* Arsenic Directly Binds to and Activates the Yeast AP-1-Like Transcription Factor Yap8. *Molecular and Cellular Biology* **36**, 913–922 (2016).

156. Zhou, X. *et al.* Arsenite Interacts Selectively with Zinc Finger Proteins Containing C3H1 or C4 Motifs. *J. Biol. Chem.* **286**, 22855–22863 (2011).

157. Bian Zhou-Yan *et al.* LIM and Cysteine-Rich Domains 1 Regulates Cardiac Hypertrophy by Targeting Calcineurin/Nuclear Factor of Activated T Cells Signaling. *Hypertension* **55**, 257–263 (2010).

158. Sica, A. *et al.* Interaction of NF-κB and NFAT with the Interferon-γ Promoter. *J. Biol. Chem.* **272**, 30412–30420 (1997).

159. Serfling, E. *et al.* NFAT and NF-κB factors—the distant relatives. *The International Journal of Biochemistry & Cell Biology* **36**, 1166–1170 (2004).

160. Erlanson, D. A., Chytil, M. & Verdine, G. L. The leucine zipper domain controls the orientation of AP-1 in the NFAT·AP-1·DNA complex. *Chemistry & Biology* **3**, 981–991 (1996).

161. Fujii, T. *et al.* Gα12/13-mediated Production of Reactive Oxygen Species Is Critical for Angiotensin Receptor-induced NFAT Activation in Cardiac Fibroblasts. *J. Biol. Chem.* **280**, 23041–23047 (2005).

162. Huang, C. *et al.* Hydrogen Peroxide Mediates Activation of Nuclear Factor of Activated T Cells (NFAT) by Nickel Subsulfide. *Cancer Res* **61**, 8051–8057 (2001).

163. Ke, Q. *et al.* Essential role of ROS-mediated NFAT activation in TNF-α induction by crystalline silica exposure. *American Journal of Physiology-Lung Cellular and Molecular Physiology* **291**, L257–L264 (2006).

164. Krege John H., Hodgin Jeffrey B., Hagaman John R. & Smithies Oliver. A Noninvasive Computerized Tail-Cuff System for Measuring Blood Pressure in Mice. *Hypertension* **25**, 1111–1115 (1995).

165. Feng, M. *et al.* Validation of Volume–Pressure Recording Tail-Cuff Blood Pressure Measurements. *Am J Hypertens* **21**, 1288–1291 (2008).

166. Drobná, Z., Walton, F. S., Harmon, A. W., Thomas, D. J. & Stýblo, M. Interspecies Differences in Metabolism of Arsenic by Cultured Primary Hepatocytes. *Toxicol Appl Pharmacol* **245**, 47–56 (2010).

167. Mordukhovich, I. *et al.* Association Between Low-Level Environmental Arsenic Exposure and QT Interval Duration in a General Population Study. *Am J Epidemiol* **170**, 739–746 (2009).

168. Dhar, P., Kaushal, P. & Kumar, P. Antioxidant supplementation upregulates calbindin expression in cerebellar Purkinje cells of rat pups subjected to post natal exposure to sodium arsenite. *Brain Research* **1690**, 23–30 (2018).

169. Gurr, J.-R., Liu, F., Lynn, S. & Jan, K.-Y. Calcium-dependent nitric oxide production is involved in arsenite-induced micronuclei. *Mutation Research/Genetic Toxicology and Environmental Mutagenesis* **416**, 137–148 (1998).

170. Phan, N. N., Wang, C.-Y. & Lin, Y.-C. The novel regulations of MEF2A, CAMKK2, CALM3, and TNNI3 in ventricular hypertrophy induced by arsenic exposure in rats. *Toxicology* **324**, 123–135 (2014).

BIOGRAPHICAL SKETCH

August 11, 1996.....Born, Fort Lauderdale, Florida

June 13, 2014.....Diploma, South Burlington High School, Vermont

May 24, 2018.....B.S. Molecular & Cellular Biology, Johns Hopkins University, Maryland

May 19, 2020.....Sc.M. Toxicology & Pathophysiology, Johns Hopkins University, Maryland

Raihan Kabir grew up in South Burlington, Vermont. He completed his undergraduate training in Molecular and Cellular Biology and graduate training in Human Toxicology and Pathophysiology, both at Johns Hopkins University. His research interests focus on cardiovascular science in health and disease.